Answer to the referees comments on

Ice particle sampling from aircraft –
influence of the probing position on the ice water content

by

Afchine, A., Rolf, C., Costa, A., Spelten, N., Riese, M., Buchholz, B., Ebert, V., Heller, R., Kaufmann, S., Minikin, A., Voigt, C., Zöger, M., Smith, J., Lawson, P., Lykov, A., Khaykin, S., and Krämer, M.

Correspondence to: Martina Krämer (m.kraemer@fz-juelich.de)

First of all, a great thank to all three referees for their thorough reading of the paper and their detailed comments, which helped to improve the manuscript.

We have taken into account all the points noted by the referees and included almost all of them in the new manuscript.

Reading the reports we understood that the description of the method we used and also the intention of the study was to brief and thus not clear. Hence, many of the changes in the manuscript are adding more detailed information. In particular, we have added a new section (Section 2: Methodoly) describing the approach of the study.

Further, to confirm the results from the approach of comparative IWC measurements, we have added CFD simulations around the HALO aircraft for different ice particle sizes, as desired by all referees (new Figure 14).

Our point by point answers to referees are in blue.

Answer to Ref. #1:

The subject matter of this paper is very timely and appropriate for AMT, examining how the positioning of microphysics probes affects the measured ice water content. The authors compare measurements of bulk ice water contents (IWCs) made on the roof of the aircraft fuselage against those attached under a wing of the HALO aircraft, and also compare measurements mounted on the fuselage side and bottom of the Geophysica. Based on their comparison, the authors claim that the reason the IWCs measured by the roof inlets deviate from those under the aircraft wing is caused by the shadow-zone behind the aircraft cockpit. Although the authors do provide one good piece of evidence to justify their claims (their Fig. 10 that shows how the ratios of the roof/wing IWC with the mean ice crystal size), overall I found that many of the claims made in the manuscript were not well justified by the data presented and the authors did not consider all the nuances associated with the probe positioning. Provided that the authors are able to do a more thorough job of discussing the limitations of their findings and provide better justification of their conclusions, I feel that this paper should be ultimately accepted by AMT.

1. The first major problem with the manuscript is that the authors overly simplify the discussion of the flow around an aircraft and the impact of the positioning of the probe. Although their Fig. 1 (adapted from King 1984) is a great illustration of the conceptual flow around an aircraft, it is important to note that the King (1984) calculations show that for the three different aircraft shapes they examined that the width of the shadow zone and the concentration enhancement factors could be described in terms of the scaled fuselage radius and a parameter similar to the Stokes number. I did not see anywhere in this paper where the authors discussed the expected location of the shadow or enhancement zones based on the fuselage radius or this 'Stokes parameter' for either the HALO or Geophysica. It would seem that such a calculation would be required to justify their conclusions. Note, that ideally a complete flow analysis around the aircraft would be completed, but I am aware that such an analysis would be well beyond the scope of the paper. However, this later calculation would be something well within what would be expected for the scope of this paper.

   We have performed now CFD calculations (showing the enrichment and shadow zones of the HALO aircraft) that justifies our conclusions – see new Figure 14 and extended Section 5.2 (old section 4.2).

2. Second, the authors make no comments about the position of the probe away from the fuselage, above the roof, or underneath the wind of the aircraft. Knowing this location is very critical to determining whether the probe is in an enhancement or shadow zone. For example, probes underneath an aircraft wing that are either not far enough below the wind or not far enough ahead of the leading edge of the wing might also suffer some large effects from the flow around the aircraft. The authors have included no discussion about this whatsoever in their paper. First, I think more details about the mounting location of the probes are required, and this position should be assessed in terms of the expected location of the shadow/enhancement zones from the King (1984) type analysis.

We have included the exact positions of the probes into Section 4 (old Section 3). A discussion on effects that can influence IWC measurement (except of roof sampling) is introduced in the new Sections 2 (Methodology).

3. Third, I see that the scatter between the IWC derived from the side and wing-mounted probes of a factor of 2.5 quite large. Further, the scatter can go even beyond this mean 2.5 figure. This seems extremely large to me. What is the uncertainty of the IWCs that are measured by these probes? Is it as large as a factor of 2.5? If less, what is causing the large amount of scatter? There needs to be more thorough uncertainty analysis than is currently presented in the paper.

   A more detailed discussion is now presented in new Section 5.1.4 (Scatter of IWC measurements).

4. Fourth, the authors attribute the differences they are seeing to the locations of the different probes. I agree that this seems to be the most likely reason for the differences. But, it would seem that to properly attribute this to the location of the probes, experiments should have been performed where the probes were switched between the different positions to see that the same order of differences still occurred. Is such a switch possible given the mounting possibilities on the aircraft?

   The referee is right that switching instruments at the same plane would be the ultimate proof of the conclusion that the roof sampling position is causing the differences in the IWC measurement. Unfortunately, this is impossible on HALO. However, on board of Geophysica, we operated the same instrumentation (FISH and NIXE-CAPS) as on HALO, but with side mounting for the total water measurement (this is now mentioned in the Section 5.1.3 - old 4.1.3). Further, FISH is used on the WB-57 at the bottom of the plane, so we have the same instrument for the total water measurements on three aircraft (and two very similar cloud probes for the PSD_{ice} measurements).

   To better explain the method that we have used to evaluate and quantify differences our IWC measurements on aircraft, we have introduced a new Section (Section 2: Methodology).

5. Fifth, the authors need to do a better job in characterizing the uncertainty associated with the derivation of IWCs associated from size-resolved measurements through the use of m-D relations. Whereas the authors do acknowledge these uncertainties, noting that the bulk IWC is less error-prone in comparison to the IWC from the PSD, I feel that they are rather premature in making the claim that their m-D relation has demonstrated the robustness of their connection between cirrus ice crystal size and mass. This again seems a bit suspect given the difference of a factor of plus or minus 2.5. This also seems quite large compared to some other studies that have studied the variance of m-D relations in how they are related to calculations of bulk IWC and comparison with that derived from size distributions. How would the use of other m-D relations compare? Would some also work within the 2.5 factor or would they be smaller/larger? These issues need to be addressed especially if a conclusion is going to be made that 'the agreement of the IWCS . . . demonstrates the validity of the m-D relation of Erfani and Mitchell (2016), slightly modified by Kramer et al. (2016) and Luebke et al. (2016).' There can be variations in

m-D relations as the particle habits and densities can change not only with temperature, but also with the type of cloud being sampled.

We have added a Figure (new Figure 8) to new Section 4.2 (old 3.2: Cloud spectrometers for IWC) showing that the use of other m-D relations will not greatly alter the IWC calculations. We think that Figure 8 together with the discussion of the scatter and significance of IWC measurements in the new Sections 2 and 5.1.4 now makes the conclusions drawn in the paper more sound.

6. Finally, I think it is also very important that the conclusions made are specific. The authors may want to claim for that the particular probes mounted on the specific aircraft at the specific locations, there are certain things that can be said about preferred mounting locations. However, there simply is not sufficient evidence to generalize these findings to mounting locations on aircraft in general, or to locations in general (below wing, on roof, on fuselage, etc.)

   We have deleted generalizing statements in the manuscript. However, I do not fully agree with the referee here. What we have shown with the measurements -and now also with CFD calculations- confirm the current knowledge from experimental and theoretical work, that means it is not only very specific for these aircraft or instrumentation. What is specific here are the size ranges and strength of ice particle enrichment or losses on the planes roof.

Other Comments:

7. Page 5, line 19, What is sufficient distance?

   ' ... sufficient distance ... to minimize particle losses or enrichment due to distorted cloud particle trajectories ...'
   The distances for the deployed instrument are now given in Table 1.

8. Page 7, line 30: Was there any precipitation probe? What did the mass distribution function look like? Is there any possibility some mass is being missed in the IWC from the lack of particles above 937 micrometers being measured? Even if such particles are contributing minimally to the number, they can contribute more substantially to the mass.

   No, the was no precipitation probe on board. And as can be seen from Figure 13, in most cases the particle sizes do not exceed 1000 μm - which is typical for cirrus clouds. In cases with larger ice crystals you are right - then the losses in IWC from PSD_{ice} are even larger. These cases happen mostly at the warmer cirrus temperatures ($>$ 230 K), where liquid origin cirrus dominates.

Answer to Ref. #2:

General Comments:

Measurements of ice water content at different aircraft mounting locations are potentially of interest, since much of current knowledge is based on potential flow or CFD models. It's a start, but this paper needs major revisions before it is publishable. The presentation is confusing, and much of the introductory material (including objectives) lacks focus and clarity. Also, the paper seems incomplete without additional work that is needed to quantify and scale each fuselage position for different aircraft. My specific suggestions are below.

Specific Comments:

1) There is very awkward English used throughout. Please avail yourself of an English AMTD editing service.

We will do this at the final stage of the production process by AMTD.

2) Abstract line 3-8: Please clearly explain that you are comparing upper fuselage vs wing measurements on one business-jet aircraft from one experiment, and separate comparisons on specialized high-altitude aircraft from different experiments. The various aircraft wing and cockpit geometries are very different, and not everyone will know that HALO is a Gulfstream G-V, or what the Geophysica and WB57F are.

We have specified the aircraft types of the different field experiments.

3) Abstract line 20: A 'factor of 2.5' doesn't sound like good agreement, and may be misleading as actually the vast majority of your data points are much better than that. I recommend finding a better way of quantifying the data comparisons (see also point 17).

The factor of 2.5 is explained in more detail in the new manuscript in Section 4.1.4.

4) Page 2, line 1-2: Or 'solid measurements' could also be made with an instrument mounted in a wingpod with extending inlet.

This sentence is deleted.

5) line 18: You can and should discuss the width of the shadow zone for each aircraft, based on the King (1984) modified Stokes parameter. Granted this is an estimate, but it will give an idea of the expected variance for different aircraft fuselage sizes and stations (distance back) on the aircraft. Ice crystal sizes and can be converted to aerodynamic diameters and modified Stokes parameter for typical crystal sizes and shapes.

We have introduced a new section (new 2. Methodology) where we discuss in more detail the approach we used here to address the quality of IWC measurements at different probing positions. In this section and, more detailed in Section 5.2 (old section 4.2), it is shown that from deviations of IWC measurements at the fuselage in comparison to wing IWC measurements it is possible to draw conclusions on the manner of possible IWC distortions, for example if the probing position is placed in a shadow or enrichment zone.

Since the method of comparative IWC measurements shows whether an inlet is placed in the shadow zone, without determining specifically the width of the zone of the aircraft, we feel that it is beyond the scope of this work to discuss the width of the shadow zone for each aircraft geometry.

Nevertheless, we have calculated the modified Stokes parameter provided by King (1984). Unfortunately, we found that the calculations are not applicable for the high cruising speeds of the planes involved in this study, since the angle of attack is not considered in that formulation.

Instead, we have included exemplary CFD simulations of gas streamlines and ice particle trajectories of different sizes around the HALO aircraft (new Figure 14) to demonstrate that our findings about shadow and enrichment zones using comparative IWC measurements are confirmed by the simulations.

6) lines 20-25: As in the Abstract, what measurements are being compared on which aircraft is confusing. You can't necessarily generalize from one aircraft to another. Please be specific.

See answer to 5)

7) Page 3, line 24: Every inlet will influence the airflow somewhat. So, switch 'not influence' to 'minimally influence'.

Done.

8) Page 4, Section 2.1.2: Not sure that all this detail is required; you could just specify the uncertainty/detection limits for each instrument and reference papers for more information.

It might be that this detail is not entirely essential. On the other hand, to my knowledge the relation between the enhanced total water and IWC and also detection limits are not described in detail elsewhere, and since we aim to do that we prefer to keep this section in the manuscript.

9) lines 18-23: If you are going into all this detail, a figure would be helpful. Or the section could be cut.

Thank you for this suggestion, we have added new Figure 2.

10) Lines 31-32: Only if the flow rate is not controlled, which it can be in some flow configurations.

We have noted that now.

11) Page 5, line 1: This seems backwards, since you are solving for IWC.

We have removed the confusing part of the sentence.

12) Line 8; too much detail; not sure why all this is worthy of note for this paper.

We added the following sentence to better explain why this detail is necessary: 'Because of this, the IWC detection limit as well as the uncertainty of IWC improves with decreasing temperature.'

13) Line 21, insert 'for particle measurements' after 'flow around wings', as obviously the airflow is critical for other things (like lift).

Done.

14) Page 6: line 13-14: A philosophical point: it's already known that the top of the fuselage is a bad place to sample clouds, so why were all these instruments mounted here? Are they primarily to measure gas-phase composition, with cloud measurements just for this study?

The inlets are primarily mounted at the top for gas-phase measurements. Unfortunately, when the aircraft was first deployed, no special cloud inlets were installed, so here we would like to quantify the impact of the probing position on the IWC.

15) Specify the distances from fuselage and fuselage station (distance back) for each inlet position.

We have inserted Table 1 listing all distances.

16) Page 8: line 13-14: but HAI is actually closer to fuselage, right? How much?

Yes HAI is 5.5cm closer to the fuselage - see Table 1.

17) Line 15: Actually it seems only a small fraction of measurements differ by 2.5. This should be reworded for quantitatively, and to make it clear that actually most data that fall within smaller ratios.

We have drawn the 2.5 lines in new Figure 9 so that it can be better seen now that most of data points are within that range.

And many of these are at small IWCs, and likely influenced by higher uncertainties at low values (due to subtracting a relatively large clear air signal, and possibly calibration uncertainties). This should be discussed. Likewise with the factor of 10 later on.

The uncertainties are smaller at lower IWC, because the clear air signal decreases with temperature, see new Figure 3 and Section 3.1.2.

Also, are the data from different instruments synced precisely?...as this can also increase scatter.

The different instruments are precisely synced.

18) It would also be nice to know if the different instruments have been successfully compared in the lab, a wind tunnel or in past aircraft campaigns.

Unfortunately we had not the chance to compare all instruments before. However, FISH has been compared to a number of other instruments at the cloud chamber AIDA (see Fahey et al., 2014) and on aircraft (see Rollins et al., 2014). A review of two decades of successful measurements with FISH is given by Meyer et al. (2015). This is now mentioned in the manuscript at the beginning of new Section 5.1.1.

19) Page 9: Again, we need to know how far out and back each inlet is.

This is now given in new Table 1, which is also mentioned in the text.

20) Lines 10-11: The Geophysica is also a narrower aircraft. Cannot compare directly with the G-V without scaling somehow.

In the new Section 2 (Methodology) we have now better described the approach of comparative IWC measurements. One advantage of this approach is that all effects that influence IWCs, the aircraft shape and inlet positions included, are contained in the measurements.
Hence it seems very unlikely that the different widths of the aircraft is the reason of the derivations of the IWCs, especially when at the same time these derivations look as expected if an inlet is placed at the aircraft's roof.

21) Page 10: lines 8 on: This is interesting, but it should be clarified that at very large sizes, particle trajectories are straight and little enhancement or shadowing is expected (ie, high S values for King, 1984). It appears this is outside the range of what you sampled, although it's difficult to know since S values aren't calculated.

The CFD calculations we have performed include particles of 500 μm, see new Figure 14. The discussion in Section 5.2 is extended and includes these large ice crystals.

22) Page 12: Lines 7-8: This is simplistic and dangerously misleading, since there is still a shadow zone on the side and bottom of the fuselage – it's just more narrow than on the top. It also will vary with fuselage diameter and distance behind the nose. Again, precise inlet locations are needed.

That you for mentioning that - we have extended the recommendations to that effect.

23) Need to reference prior work. Lines 15-16: Twohy and Rogers (J. Atmos. Ocean. Tech, 1993) also reported deviations in measured cloud properties for different aircraft mounting locations. Lines 18-20: Davis et al (JGR, 2007) also compared IWC measurements on the WB57F.

Thanks again, these papers are referenced now in the manuscript (Davis et al., 2007, in the new Section 5.1.4 'Scatter of IWC measurements'; Twohey et al., 1993, in Section 3.1.1 'IWC enrichment or loss due to inlet position').

Answer to Ref. #3:

Overview: This work examines the important problem of the effects of a probe's location on an aircraft, on the accuracy of its measurements. This topic has a long history of research, and has been explored since the mid-70s by different groups (e.g. Norment and Zalosh, 1974). The most well-known studies in this area were published in a series of papers by Warren King in the mid-80s. Based on the theoretical analysis of particle trajectories followed by in-situ verification (King, 1984; King et al. 1984), it was concluded that the particle number and mass concentrations can be biased by an order of hundreds of percent depending on the mounting location of the probe on the fuselage of the airplane. One of the important outcomes of the King's studies is the identification of the regions with enhanced and reduced concentrations of cloud particles at the top of the fuselage. The most favorable places for bulk microphysical instrumentation installation on the fuselage would be the side and bottom positions. This rule has been followed by many research groups when instrumenting research aircrafts for cloud microphysical measurements. The present study reiterates King's conclusion, that the cloud microphysical measurements (specifically IWC) at the side and bottom fuselage locations are more accurate compared to the top location. So, in this regard, this study confirms the existing knowledge about the preferential fuselage locations of the bulk microphysical instruments. In the present work, the conclusion about the accuracy of IWC measurements was obtained based on the comparisons of the TWC probes mounted on the different fuselage locations: top, side and bottom. Even though I agree with the conclusions of this paper, the methodology of the approach employed in this study leaves many questions unanswered. Additionally, critical components of the study of the probing positions are missing: for example, there is no assessment of the dimension of the shadow zone and its distance from the fuselage, the effect of the air density of the particle trajectories and size of the shadow zone is not accounted for, the ice concentration enhancement around the fuselage due to ice bouncing is not accounted for, the particle trajectory analysis has been omitted.

In my opinion, this study should be eventually published. However, in its present form the paper is not suitable for publication in AMT. At this stage I would suggest withdrawing the manuscript and adding the missing necessary components. Because of the great importance of the considered question, and the large anticipated impact of this work on the cloud instrumentation community, I would encourage the authors to address the questions listed below and resubmit the manuscript.

Major comments:

1. This paper validates the conclusion of the King et al (1984) study on a different instrumental basis. Further progress can be achieved by utilizing flow simulations and particle trajectory analysis. At present, CFD analysis is routinely used by different research groups (especially in the aviation community) to analyze the particle trajectories for different aspects of aviation safety and to study the accuracy of measurements of cloud microphysical instrumentation (e.g. Weigel et al., AMT, 2017). It would be highly beneficial for this paper to include these types of simulations. This will help in addressing many aspects of the positioning of the cloud microphysical instrumentation, and provide estimates of the accuracy of measurements. The CFD

and particle trajectory analysis may take some time. However, the obtained results will be rewarding for the community.

We have included CFD simulations of gas streamlines and ice particle trajectories of different sizes around the HALO aircraft (new Figure 14, Section 5.2). Further, we have added a new section to the manuscript (Section 2: Methodology) to better explain the approach of comparative IWC measurements we used here. In this section, also the application of CFD simulations to evaluate especially IWC measurements are discussed.

2. The dimensions of the shadow and enhancement zones at the mounting location of the TWC probes of the HALO aircraft should be provided here. At that stage it is not clear whether the TWC inlets were located inside the shadow zone, enhancement zone or in the relatively undisturbed free flow. Without such information, the discussion is incomplete.

The shadow and enrichment zone of the HALO aircraft is shown in the new Figure 14.

3. King (1984, part 1) considered the formation of the shadow zone on the top of the fuselage for liquid droplets. Liquid droplets after the impact with the fuselage stick to its surface and shed downstream (see Fig.6 in King, 1984, part 1). However, ice particles after impact with the fuselage rebound back into the airflow. Ice particles, after the first rebound, may experience multiple bouncing. This phenomenon was observed in wind tunnels and is well reproduced in CFD simulations (e.g. Korolev et al JTECH, 2013). One of the consequences of this effect is an enhanced concentration of ice particles around the fuselage including side and bottom locations. This is results in a principal difference compared to the King's (part 1 and 2) work, which was focused on the trajectories of liquid droplets. In this regard, it is important to consider the enhancement of ice concentration not only at the top of the fuselage, but all the way around it. This effect may equally affect IWC measurements at the side and bottom locations. This question should be properly addressed.

We address the point of ice particle bouncing in the new Section 2 (Methodology). We have not performed CFD calculations that consider bouncing, since one advantage of the approach of comparative IWC measurements is that all effects influencing IWCs, including ice crystal bouncing, are contained in the measurements. We argue that, as soon as the ice particle sampling at one or both probing positions is seriously disturbed, the IWC measurements will differ significantly from each other. Hence, a reliable agreement between IWCs from two different instruments mounted at two different positions is a reasonable indication for an applicable IWC measurement. Smaller effects influencing IWCs result in the observed scatter of the IWCs which is discussed in the new Section 5.1.2.

4. CFD simulations showed that particle trajectories are sensitive to air density air. Therefore, the dimensions of the shadow and enhancement ice particle zones depend on the air density air along with other parameters such as TAS, AoA, etc. This is a very important issue and it should be properly addressed in this study. Could you also comment on the effect of air on the dependences of IWC ratio vs Rice shown in Fig.10?

We are aware of the effect of the density of air on particle trajectories and thus the shadow and enrichment zones and note that now in Section 2 (Methodology). However, we feel that a discussion of this effect (also with respect to the IWC ratio vs Rice shown in new Fig. 12) is beyond the scope of this study. Our main aim here is the evaluation of IWC measurements on aircraft by means of the comparative approach described now in Section 2. As outlined in the previous point (3.), one advantage of the approach of comparative IWC measurements is that all effects that seriously influence IWCs, including also the effect of air density, would appear significantly in the measurements.

5. Page 10. The equation mean mass radius Rice = IWC/Nice should be written as

Rice = (3IWC/4πice Nice)ˆ 1/3.

I believe this a typo. Unfortunately, no information about ice was provided in the text. Since the size-to-mass parametrizations

M=aRiceˆ b

was applied for the IWC calculation, then ice is a function of Rice, i.e.

ice = 3aRiceˆ (b-3)/4π.

Therefore, the mean mass radius should be calculated as

Rice = (IWC/aNice)ˆ 1/b.

Could you please clarify how Rice was calculated?

R_{ice} was calculated as $\left(\frac{3 \cdot IWC}{4\pi\rho \cdot N_{ice}}\right)^{1/3}$ with $\rho = 0.92$ g/cm^{-3} and we have changed the equation accordingly.

6. It is important to indicate the distance of the TWC probes inlets from the fuselage and from the nose of the airplane. This is necessary to understanding the effect of the probe's location on the accuracy of its measurements. Along this way, it would be beneficial to include a summary table with the positioning of the TWC probes, type of the airplane, name of the project, TWC probe, particle probe used as a reference, etc.

We have included a table containing all necessary information in the manuscript (Table 1).

7. The diagrams in Figs 7, 8, 9 in their present form visualize the scattering of the IWC points. However, it is difficult to judge about the biases and the degree of scattering of the data points. It is suggested to add a linear regression line, indicate a relevant linear equation, standard deviation, and correlation coefficient in each diagram. This information will help to quantify of the degree of agreement between the IWC measurements. Please also provide the averaging time used for the data these diagrams.

We have calculated IWC-IWC linear regression and correlation coefficients, except for the Roof/Wing measurements on HALO (new Figure 10), since there is no correlation between the roof and wing IWCs. We have indicated the correlation coefficients in the plots and the coefficients in the figure captions. However, we have not plotted the regression lines into the graphs, because the graph will beome visually too confusing together with the frequencies and 1:1, 1:10 and 1:2.5 lines..

The time resolution of the measurements is now stated together with the instrument descriptions in Sections 4.1.2 and 4.2.

8. The IWC calculated from the cloud particle probes (CAS-DPOL, CIP-G,2DS) was used as a reference for the TWC probes (FISH, HAI, Waran) measurements.

The IWC from the cloud spectrometers is not used as a reference, our approach is to evaluate the IWC measurements by a comparative assessment, as now described in the new Section 2.

The processing of the scattering and imaging probes are sensitive to the algorithms and assumptions employed in the processing software. Thus, CAS-DPOL is usually calibrated in assumption that the cloud particles are spherical water droplets. Were any corrections for ice applied for the CAS-DPOL data?

We have calculated the size bins of the CAS-DPOL under the assumption of aspherical particles and found the expected differences. However, after merging the new bins for Mie ambiguities, the differences between the bin sizes between spherical and aspherical particles was so small that we decided to use only one set of size bins. This is described in Meyer et al. (2012).

What algorithms and corrections were used during the processing of the 2D probe's data?

We have used an inter arrival time algorithm to account for particle shattering and also rejection schemes for out of focus, end diode and streaker particles. This is described in detail in Meyer et al. (2012) and Luebke et al. (2016). We have referenced these papers now in the new Section 4.2.

What are the typical, min, and max number of particles in the CAS, CIP and 2DS data? Please provide an assessment of the statistical significance of PSDs used for the IWC calculations. Statistically insignificant PSDs may result in large random errors in IWC calculations. These questions should be elaborated upon and explained in the text. The assessment of the errors in the IWC calculations for the particle probe data should be provided as well.

Good point, this might be another source contributing to the scatter of IWC measurements, because due to the nature of cirrus clouds - thin, cirrous - their particle statistics is never satisfying. We mentioned that now in the new Section 2.
To achieve a better PSD_{ice} statistics, a much larger aircraft instrument sampling volume would be needed, which is beyond current technology. The other way to enhance the particle counts would be to chose longer averaging times. However, then the already low resolution in space is further reduced and cloud free areas might be assigned to clouds - we decided here to keep the high time/space resolution and accept a reduced statistical significance. We don't know the exact values the referee asks for, but we provided the total number of IWC data points in new Figs. 9, 10 and 11, they range between about 7000 and 54000 data points.
Nevertheless, a reasonable indication that large random errors in IWC caused by bad counting statistics of the particles does not greatly influence the IWC derived from the PSD_{ice} is again the scatter of IWCs observed Figs. 9 and 11 with most of the points close to the 1:1 line.

9. The diagrams in Fig.10 are supportive of the statement about oversampling of small particles and undersampling of large particles at the roof location. Similar diagrams should be provided for the side and bottom locations of the TWC inlets on Geophysica and WB57. Otherwise, one could argue that the 'duck' type behavior of the IWC ration vs Rice is a result of the errors in calculations of IWC from the particle probes.

With the more detailed explanation of the methodology (Section 2) we used here, we hope it is clear now that the 'duck' type behavior of the ratio IWC/R_{ice} is not caused by errors in calculations of IWC from the particle probes - if that would be the case then an agreement of IWC measurements (as shown in new Fig. 9) would not be possible.
Since we have already added three Figures to the manuscript (15 Figures altogether now) we decided not to provide these additional plots to again confirm our findings. Another reason is that a similar Figure cannot be produced for MacPex, because the total number of ice crystals starts is only available for crystals larger than 15 μm (instead of 3 μm), thus the mean mass size cannot be calculated.

10. Page 4, Line 15: 'However, isokinetic sampling (= the flow inside the inlet is the same as in the free flow), which in principle enables the undisturbed measurement of H2Otot, is not possible for fast flying aircraft, since the air flow speed is always much higher than the velocity inside of the inlet.' The airborne version of the isokinetic probe for measurements of cloud condensed water was designed by NRC: (Davison, C., J. MacLeod, J. Strapp, and D. Buttsworth, 2008: Isokinetic total water content probe in a naturally aspirating configuration: Initial aerodynamic design and testing. Proc. 46th AIAA Aerospace Sciences Meeting and Exhibit, Reno, NV, American Institute of Aeronautics and Astronautics, AIAA 2008-435. [Available online at http://arc.aiaa.org/doi/abs/10.2514/6.2008-435.]) This probe was successfully operated during several field campaigns on different aircrafts. Some results were published in JTECH.

The sentence is changed to 'However, as explained in the following, a deviation of the gas streamlines is desirable when sampling cirrus clouds, since cirrus are very thin and their IWC correspondingly small. To this end, so called 'nearly virtual impactors' (see Figure 2) are used for the collection of cirrus ice particles. ...'

11. Traditionally, condensed water content is measured in g/m3 (liquid, ice or total water content) or g/kg (mixing ratio). These units are well adapted by the cloud and climate modeling communities (both g/m3 and g/kg), remote sensing community (g/m3), aviation industry (mainly g/m3). The present paper is utilizing non-conventional units in the cloud physics community (ppmv) in order to describe condensed water content. This unit is usually used to describe concentration of a gas phase, rather than to characterize the weight of a liquid or solid phase per unit volume. This unit is mainly employed by the subcommunity formed around the evaporators used for measurements of the condensed cloud phase (e.g. FISH, HAI, Waran, etc.). I am not sure that employing this unit adds clarity; rather, it creates barriers in the dissemination of the IWC measurements that employ this unit. In my opinion, the cloud and climate modeling communities and the remote sensing community are unlikely to switch to this unit. The aviation industry is quite conservative, and it most likely they will ignore the measurements of condensed water content in this unit. I recommend using the conventional units of g/kg or g/m3. At minimum, I suggest using additional axes with conventional units in Fig. 7, 8 ,9, 10.

We are aware that traditionally g/m^{-3} is used as unit for condensed water and account for that in new Figure 3, where we show IWC vs. temperature in both units, ppmv (volume mixing ratio) as well as mg/m^{-3}. The reason that we prefer volume mixing ratios is that it is a conserved quantity, i.e. they do not change with temperature and pressure and are therefore better comparable with each other. In our publications, we use to show a graph with two panels, one for each unit, here Figure 3.

Minor comments:

1. Page 2, Line 11: 'The IWC of a cirrus is a bulk quantity which is composed of the sum of all ice particles. . .' The term 'of a cirrus' is redundant here. This statement is relevant to any cloud, not just cirrus.

Changed.

2. Page 2, Line 11: It should be '. . .the sum of all ice particles masses. . .'

Changed.

3. Page 2, Line 15: 'In particular, King (1984) shows that above the roof of an aircraft the sampling of particles is disturbed.' Strictly speaking, the sampling of particles is disturbed everywhere around the fuselage. However, the scale of this disturbance is different. Please reword this sentence.

Changed.

4. Page 2, Line 16: 'However, to simulate and quantify losses or enrichment of ice particles and the effect on IWC at a specific position of an aircraft is hardly possible, since this depends on the prevailing particle size distribution and also the irregular shape of the ice crystals.' This is a too strong of a statement. The irregular ice particle shapes can be replaced with spheres with equivalent aerodynamic size. For example, particle trajectory analysis can be performed using spheres with the mass density calculated from size-to-mass parametrizations M=aDˆ b.

The sentence is changed to 'However, to simulate and quantify losses or enrichment of ice particles and the effect on IWC at a specific position of an aircraft is hardly possible, since this depends on the prevailing ice particle size distribution and also th flight conditions.'

5. Page 2, Line 27: 'The IWC of cirrus can be recorded from aircraft either by bulk cloud measurements using airborne closed path hygrometers mounted behind an inlet tube or via integration of the ice particle number size distributions (PSDice) measured by cloud spectrometers. In both cases, the ice particles must be properly sampled before the measurement.' Hot-wire probes are missed in this statement.

We did not mention hot-wire probes because this technique is not to be recommended for ice crystals because the crystals bounce from the wire.

6. Page 2, Line 29: 'The bulk IWC is less error prone in comparison to the IWC from PSDice in case of an undisturbed measurement.' This is a questionable statement. Both techniques have its own problems and advantages.

The sentence in changed to 'The bulk IWC is less error prone in comparison to the IWC from PSDice in case of undisturbed ice particle sampling.'

7. Page 3, Line 1: replace 'Fore' to 'For'.

Changed

8. Page 3, Line 18: ‘To precisely detect H2Otot’ replace by ‘To precisely measure H2Otot’

We have changed the sentence to ‘To precisely determine H2Otot’ to avoid to use ’measure’ too often.

9. Page 4, Line 6: ‘To specify the size ranges of the ‘smaller’ and ‘larger’ cloud particles, CFD calculations for the specific conditions of fuselage shape, aircraft speed and inlet distance from the nose of the aircraft need to be performed.’ This sentence is disconnected from the following text and it appears to be redundant.

The sentence is changed to ‘To specify the aforementioned size ranges of the ‘smaller’ and ’larger’ cloud particles, CFD calculations for the specific conditions of fuselage shape, aircraft speed and inlet distance from the nose of the aircraft need to be performed.’ to make clear that it refers to the previous text.

10. Page 4, Line 7: ‘Very roughly, cloud particles with radii $<30\mu$m can be assumed to belong to the smaller, while those $>30\mu$m are associated to the larger part of the cloud particle size spectrum at jet aircraft with high air speeds.” What is the basis for this statement? References should be provided here.

The basis for this statement is this study, thus there is no reference.

11. Page 4, Line 23: “. . .shattering into small artifacts at the cloud probes head. . .” should be “. . .shattering into small fragments at the cloud probes’ housing. . .”

The sentence is changed to ’Ice crystal shattering into small fragments at the cloud probes head ...’

12. Page 4, Line 23: “However, for the calculation of the IWC, the uncertainty from shattering does not play a significant role since the shattered crystals still contribute to the integrated mass of PSDice.” This sentence should be reworded.

The sentence is changed to ’However, it (shattering) does not play a significant role for the calculation of the IWC, since the ice fragments contribute to the integrated mass of PSD_{ice} in the same way as the original large crystal.

13. Page 4, Line 9: IWCS should be IWCs

There is no ‘IWCs’ at this place, I guess you mean Page 5, Line 10 $\rightarrow$ changed.

14. Figure 11. The y-labels are not easily legible. Please enlarge the font size.

Changed.

Ice particle sampling from aircraft – influence of the probing position on the ice water content

Armin Afchine[1], Christian Rolf[1], Anja Costa[1], Nicole Spelten[1], Martin Riese[1], Bernhard Buchholz[2], Volker Ebert[2], Romy Heller[3], Stefan Kaufmann[3], Andreas Minikin[3], Christiane Voigt[3], Martin Zöger[3], Jessica Smith[4], Paul Lawson[5], Alexey Lykov[6], Sergey Khaykin[7], and Martina Krämer[1]

[1]Forschungszentrum Jülich, Institute of Energy and Climate Research (IEK-7), Jülich, Germany;
[2]Physikalisch-Technische Bundesanstalt Braunschweig, Germany
[3]Deutsches Zentrum fr Luft- und Raumfahrt, Institute for Physics of the Atmosphere, Oberpfaffenhofen, Germany
[4]Harvard University, Cambridge, MA, USA
[5]SPEC Incorporated, Boulder, CO, USA
[6]Central Aerological Observatory (CAO), Department of Upper Atmospheric Layers Physics, Moscow, Russia
[7]LATMOS/IPSL, UVSQ Université Paris-Saclay, UPMC University Paris 06, CNRS, Guyancourt, France

Correspondence to: Martina Krämer (m.kraemer@fz-juelich.de)

Abstract. The ice water content (IWC) of cirrus clouds is an essential parameter determining their radiative properties and thus is important for climate simulations. Therefore, for a reliable measurement of IWC on board of research aircraft, it is important to carefully design the ice crystal sampling and measuring devices. During the ~~HALO field campaign ML-CIRRUS~~ ML-CIRRUS field campaign in 2014 with the German Gulfstream GV HALO (High Altitude LOng range) aircraft, IWC was recorded by three closed path total water together with one gas phase water instrument. The hygrometers were supplied by inlets mounted on the roof of the aircraft fuselage. Simultaneously, the IWC is determined by a cloud particle spectrometer attached under an aircraft wing. Two more examples of simultaneous IWC measurements by hygrometers and cloud spectrometers are presented, but the inlets of the hygrometers were mounted at the fuselage side (M-55 Geophysica, StratoClim campaign 2017) and bottom (NASA WB57, MacPex campaign 2011). This combination of instruments and inlet positions provides the opportunity to experimentally study the influence of the ice particle sampling position on the IWC with the approach of comparative measurements. As expected from ~~theoretical considerations~~theory and shown by Computational Fluid Dynamics (CFD) calculations, we found that the IWCs provided by the roof inlets deviate from those measured under the aircraft wing. Caused by the inlet position in the shadow-zone behind the aircraft cockpit, ice particles populations with mean mass sizes larger than about 25 µm radius are subject to losses, which lead to strongly underestimated IWCs. On the other hand, cloud populations with mean mass sizes smaller than about 12 µm are dominated by particle enrichment and thus overestimated IWCs. In the range of mean mass sizes between 12 and 25µm, both enrichment and losses of ice ~~crystal~~ crystals can occur, depending on whether the ice crystal mass peak of the - in these cases bimodal - size distribution is on the smaller or larger mass mode. The resulting deviations of the IWC reach factors of up to 10 or even more for losses as well as for enrichment. Since the mean mass size of ice crystals increases with temperature, losses are more pronounced at higher temperatures while at lower temperatures IWC is more affected by enrichment. In contrast, in the cases where the hygrometer inlets were mounted at the fuselage side or bottom, the agreement of IWCs is -due to ~~undisturbed~~ less disturbed ice particle sampling, as expected

from theory- most frequently within a factor of 2.5 or better, independently of the mean ice crystal sizes. ~~Summarizing, in case IWC needs to be detected solely by measurements from closed path hygrometers, it is crucial for a solid measurement to mount the respective inlets at the aircraft's~~ The rather large scatter between IWC measurements reflects for example cirrus cloud inhomogeneities, instrument uncertainties as well as slight sampling biases which might occur also at the side or bottom ~~.~~ of the fuselage and under the wing. However, this scatter is in the range of other studies and represent the current best possible IWC recording on fast flying aircraft.

Contents

1 Introduction

Cirrus ice water content (IWC) is directly linked to the clouds extinction and thus relates bulk cloud properties to radiative properties (e.g. Gayet et al., 2004; Heymsfield et al., 2014; Thornberry et al., 2017). Since IWC is a parameter representing cirrus in global climate models, a solid knowledge of IWC is of importance. The most accurate measurements are achieved by in-situ aircraft observations where cirrus clouds are directly probed. However, the measurements must be carried out carefully to obtain the desired data quality. Beside the ability of the instruments that are used to detect the complete range of IWCs with sufficient accuracy, the probing position at the aircraft's fuselage is of importance (see Krämer et al., 2013, and references therein).

The IWC ~~of a cirrus~~ is a bulk quantity which is composed of the sum of all ~~ice particles~~ masses of ice particles of different sizes contained in an air volume. ~~Depending on the position around the aircraft fuselage,~~ Yet there are shadow and enrichment zones for ice ~~particles in dependence of the particles size~~ crystals, which depend on the ice particle size and and the position relative to the fuselage. These zones are the most prominent particle measurement bias caused by an aircraft body. Thus, in case the position for particle sampling is placed in such a zone, it can be expected that an IWC measurement will be distorted. These effects are described already by airflow and trajectory calculations in King (1984) for different sized cloud particles. In particular, King (1984) shows that above the roof of an aircraft the sampling of particles is greatly disturbed. However, to simulate and quantify losses or enrichment of ice particles and the effect on particularly the IWC at a specific position of an aircraft is hardly possible, since this depends on the prevailing ice particle size distribution and ~~also the irregular shape of the ice crystals~~flight conditions.

Here, we ~~compare~~ use an experimental approach to determine the influence of particle probing positions on IWC measurements of cirrus clouds, by comparing in-situ observations of IWC measured at the roof, side, bottom and under the wing of aircraft with different instruments~~to evaluate the influence of the particle probing position on cirrus IWC~~. Specifically, IWC is measured under the wing - which is the most favorable position for particle sampling - during three field campaigns with differing aircraft. One aircraft is ~~in addition~~ additionally equipped with three other IWC instruments placed at the aircraft roof, at the second the IWC ~~measurements are~~ measurement is placed at the aircraft side and at the third at the aircraft bottom. From the comparison of the correlation of the roof, side and bottom to the wing IWCs conclusions are drawn about the representativeness of the ~~measurement~~ measurements at the specific position. The results of the measurements at the aircraft roof are validated by exemplary CFD simulations of gas streamlines and ice particle trajectories around the aircraft for typical conditions during penetrations of cirrus clouds.

2 Methodology

To determine the quality of an IWC measurement performed on airplanes is challenging, because the IWC evolves from a population of ice crystals of varying size that can be influenced by flow perturbations caused by the aircraft. In a perfect system, all ice particles of each size that are contained in a volume of undisturbed air would be collected. However, even small distortions of the airflow in comparison to calm air conditions can cause deviations in the IWC. These and other effects that depend on the size of the crystals can distort the IWC measurement in different ways and it is difficult to reproduce their influence on IWC.

To understand the effects that may occur for specific ice particle sizes, CFD simulations of gas streamlines and particle trajectories around an airplane are helpful. These effects can be caused for example by unfavorable sampling positions together with specific flight conditions such as the aircraft speed and the planes angle of attack. For specific cases, potential shadow or enrichment zones can be identified and the effect on IWC can be estimated. These estimates, however, differ for each particle size and, in addition, the particle concentration of each size must be known to determine the overall influence on the IWC. This influence can also vary for each IWC measurement with the ice particle size distribution (PSD_{ice}), flight conditions and related changes of the shadow and enrichment zones.

On the other hand, all effects that may occur as a result of flow disturbances or other causes (discussed in the last paragraph of this section) are included in the measurement of the bulk IWC. Hence, for the evaluation of the quality of IWC measurements an experimental comparative approach of IWC measurements is useful. The explanatory power of comparative IWC measurements is described in the following. The first step of the approach is to establish a reference bulk IWC measurement with respect to the instrument performance (i.e. good precision of the measurement). This is achieved by gas phase and total water measurements with different instruments mounted on a fuselage (see Section 5.1.1).

Next, the bulk IWC is compared to an IWC measurement at a differing position, here at the aircraft wing, which is least susceptible to flow disturbances. In this study, the wing IWC is derived from the measurements of PSD_{ice}, that should be only weakly influenced by flow perturbation effects. An agreement of the wing IWC with the bulk IWC measured on the fuselage (shown in Section 5.1.3) could indicate that both measurements are influenced in the same way by flow perturbations or instrument and other effects - but this seems not very likely because of the very different flow conditions for the sampling positions under the wing and on the roof. We interpret such an agreement in the way that both measurements are little influenced by airflow or instrument and other effects. Such a reliable agreement between IWCs from two different instruments mounted at two different positions is a reasonable indication for an applicable IWC measurement. Vice versa, as soon as the ice particle sampling at one or both positions is seriously disturbed by effects outlined in the next paragraph, the IWC measurements will differ significantly from each other (see Section 5.1.2). As will be shown in Section 5.2, from such IWC deviations it is possible to draw conclusions on the manner of the IWC distortion, for example if the probing position is placed in a shadow or enrichment zone. Also, the IWC deviations from each other can be quantified by using the comparative IWC approach.

However, some scatter between IWCs measured with different instruments and at different positions must be expected. The reasons for this are manifold: first of all, cirrus clouds are very inhomogeneous, even on a small scale, so even slightly differing probe mounting positions can cause differing IWCs. Also, each mounting position on a fast flying aircraft, even when chosen as careful as possible, might be slightly influenced by distortions of the airstream in comparison to the calm air conditions and thus can cause deviations in IWCs. Further, bouncing ice crystals may break and the small fragments may enter the IWC sampling areas and, also, the density of air can influence the particle sizes that enter these areas. Last, some unknown uncertainties are always included in the derivation of IWC from the PSD_{ice}. For example, the applied parametrizations are derived from measurements with a certain scatter, and, the particle counting statistics can be poor in thin cirrus clouds. The resulting overall scatter between IWC measured in this study is shown in Section 5.1.4.

3 IWC measurements - a brief excursion into theory

~~The~~ As introduced in the previous section, the IWC of cirrus can be recorded from aircraft either by bulk cloud measurements using airborne closed path hygrometers mounted behind an inlet tube or via integration of the ice particle number size distributions~~(~~, $\mathrm{PSD_{ice}}$~~)~~, measured by cloud spectrometers. In both cases, the ice particles must be properly sampled before the measurement. The bulk IWC is less error-prone in comparison to the IWC from $\mathrm{PSD_{ice}}$ in case of ~~an undisturbed measurement~~undisturbed ice particle sampling. The reason is that before the bulk measurements the ice crystals are evaporated while the size resolved IWC detection must account for the ice crystal shapes. In the following, a brief summary on sampling and measuring IWC on fast flying aircraft is given. ~~Fore~~ For more detail, we refer to e.g. Krämer and Afchine (2004), Schiller et al. (2008), Wendisch and Brenguier (2013), Krämer et al. (2013), Luebke et al. (2013).

3.1 IWC from hygrometers

The bulk IWC is derived from the difference between $\mathrm{H_2O_{tot}}$, which is the amount of total water ($\mathrm{H_2O_{gas}}$ + evaporated ice crystals) contained in a cirrus, and $\mathrm{H_2O_{gas}}$, the gas phase water amount. The IWC is calculated by using the following Equation:

$$\mathrm{IWC} = \mathrm{H_2O_{tot}} - \mathrm{H_2O_{gas}} = \frac{\mathrm{H_2O_{enh}} - \mathrm{H_2O_{gas}}}{\mathrm{E_{max}}} \tag{1}$$

where $\mathrm{H_2O_{enh}}$ ($\mathrm{H_2O_{tot}}$ enhanced by an oversampling of ice crystals) and $\mathrm{E_{max}}$ (enhancement factor) are parameters related to the sampling of the ice crystals by an inlet tube which is described in Section 3.1.2.

For the measurement of $\mathrm{H_2O_{gas}}$, the air loaden with water vapor is passed into the aircraft by an inlet tube which faces against the direction of flight. Therefore, a pump is used to suck the air through the inlet-hygrometer-exhaust line. No cloud particles enter backward facing inlets, since their inertia is too high for a complete U-turn. The hygrometer is mounted behind the inlet in the aircraft cabin.

To measure $\mathrm{H_2O_{tot}}$ (or $\mathrm{H_2O_{enh}}$, respectively) is more difficult, since also ice particles of a wide range of sizes (≈ 3 – 1000 µm or more in cirrus clouds) has to be passed into the aircraft. To this end, inlet tubes facing into the direction of flight are deployed. To precisely ~~detect~~ determine $\mathrm{H_2O_{tot}}$, the ice crystals have to be completely evaporated before they enter the hygrometer, which is placed subsequently in the sampling line. ~~To this end~~For that, the inlet should be heated to up to 90°C. In addition, a strong bend should follow directly behind the inlet to shatter ice crystals to small fragments that evaporate in a short time. Behind the water measurement the air leaves the aircraft at the outlet point. Most systems are so-called 'free stream' sampling lines, i.e. the flow is generated by the pressure difference between the inlet tip and the outlet. Prerequisite for a reliable $\mathrm{H_2O_{tot}}$ measurement is a suitable, well-characterized inlet so that the true concentration of water plus evaporated ice crystals can be determined. To accomplish this requirements, two points are important: (i) First, the inlet needs to be placed at the aircraft fuselage in a way to enable sampling in undisturbed flow. (ii) Further, the inlet itself should ~~not~~ minimally influence the gas phase water and ice particle concentration. These two points are briefly described in the following, mainly based on Krämer et al. (2013) and references therein.

3.1.1 IWC enrichment or loss due to inlet position

The principle behavior of gas streamlines and cloud particle trajectories around an aircraft fuselage can be seen in Figure 1 (adapted from King, 1984). In the upper panel of these early, but still meaningful potential flow simulations, the predicted gas flow streamlines at 90 m/s are displayed. Far in front of the aircraft's nose they are equally spaced, indicating the same flow velocity. However, due to the aircraft body the streamlines are compressed over the cockpit, indicating regions of higher airspeed -and also enriched concentrations of smaller cloud particles that follow the streamlines- ~~(right side)~~ compared to the free stream.

In the bottom panel, trajectories for larger (exemplarily 100 µm) cloud particles are displayed for the same flight conditions. As these particles have high inertia, most of the trajectories end at the aircraft fuselage, i.e., the particles impact on the aircraft. However, some of the trajectories were deviated, leading to regions devoid of particles (shadow zone) or with increased particle concentration (enrichment zone).

To specify the aforementioned size ranges of the 'smaller' and 'larger' cloud particles, CFD calculations for the specific conditions of fuselage shape, aircraft speed and inlet distance from the nose of the aircraft need to be performed. Very roughly, cloud particles with radii $<$30 µm can be assumed to belong to the smaller, while those $>$30 µm are associated to the larger part of the cloud particle size spectrum at jet aircraft with high air speeds. Altogether, when measuring cloud particles on the plane roof it is important to know where shadow and enrichment zones on the aircraft platform are located, since at the same fuselage station it is possible to sample in the shadow/enrichment zone for larger/smaller particles if a probe is positioned close to the aircraft fuselage or in the enrichment zone for larger particles in case the probe is farther away from the fuselage.

To minimize the effect of streamline compression and deviation of particle trajectories during the sampling of cloud particles, it is favorable to mount the sampling inlets on the aircraft's side or bottom well apart of the fuselage. There, the flow is much closer to free stream conditions, and the largest deviations from these conditions occur near the fuselage and in regions of strong curvature (Twohy and Rogers, 1993). Most favorable for an undisturbed sampling on aircraft is most likely the position under an aircraft wing, since the aerodynamically shaped wing has the least influence on the flow.

3.1.2 IWC enhancement due to inlet design

The first requirements to an inlet for a proper sampling are that it protrudes beyond the aircraft's boundary layer and that the wall of the inlet tip is thin enough to avoid strong shattering of ice crystals or deviation of streamlines from the free flow. However, ~~isokinetic sampling (= the flow inside the inlet is the same as in the free flow), which in principle enables the undisturbed measurement of , is not possible for fast flying aircraft, since the air flow speed is always much higher than the velocity inside of the inlet. Such inlet types are~~ as explained in the following, a deviation from the gas streamlines is desirable when sampling cirrus clouds, since cirrus are very thin and their IWC correspondingly small. To this end, so called 'nearly virtual impactors' ~~,~~ ~~since~~ (see Figure 2) are used for the collection of cirrus ice particles. These are inlets where the velocity inside of the inlet tube (U) is much smaller than the flow speed (U_0). Actually U is so small that the inlet cross section appears like an impaction plate. Such inlets sample strongly '~~subisokinetic~~sub-isokinetic', i.e. the part of the cross section where gas streamlines enter the inlet is much smaller than the part of the cross section that samples ice particles. The particle sampling cross sections increases with increasing particle size up to the total inlet cross section for the largest particles. As a consequence, ice crystals are sampled from a much larger (enhanced) air volume than H_2O_{gas} and thus the combined sampling of H_2O_{gas} and evaporated ice crystals is also enhanced (H_2O_{enh} instead of H_2O_{tot}). To adjust the two volumes to each other, the ice crystal air volume (and thus the IWC, see Eq. 1) needs to be corrected for this enhancement.

As mentioned, the enhancement (which can also be called 'aspiration efficiency') is dependent on particle size and increases for larger particles, up to a maximum value E_{max}. This maximum value is used for the calculation of the IWC (see Eq. 1). E_{max} can be calculated from the velocity of the free stream ~~(i.e. the aircraft speed~~ U_0 ~~)~~ and the velocity U inside of the inlet:

$$E_{max} = \frac{U_0}{U} \tag{2}$$

The point where the enhancement is 50% of E_{max} (E_{50}) is called the 'cut-off' size of the inlet which defines the particle size range sampled by the inlet. E_{max} is dependent on U, which in turn depends, among other parameters like pressure, temperature and aircraft speed U_0, strongly on the pressure difference between inlet and outlet, the driving force of the flow (in case the flow rate is not controlled). Thus, U decreases with increasing altitude.

With the knowledge of E_{max}, the IWC can now be calculated following Eq. 1~~and consequently is +IWC.~~ . In Figure 3, we visualize the complex relation between the measuring parameter H_2O_{enh}, IWC and E_{max} in dependence of temperature for given H_2O_{gas} (assumed as the saturation value for the calculations), calculated from Eq. 1 (left column: E_{max} = 10, right column: E_{max} = 50; top row: volume mixing ratio, bottom row: concentration). To avoid very small artificial IWCs caused by the uncertainties of measurements and not by ice particles, the minimum difference between H_2O_{enh} and H_2O_{gas} needs to be ~~to~~ 5% to encounter an IWC. The differently colored regions show the ranges of H_2O_{enh} and IWC belonging to each another. It can be seen from Figure 3, that the IWCs covered by H_2O_{enh} of the same color are broader and show lower IWCs at higher temperatures and narrower with higher IWCs at lower temperatures. This reflects the fact that H_2O_{gas} decreases with temperature and is thus stronger enhanced due to the addition of ice crystals. Consequently, H_2O_{enh} 'jumps' to a higher value with another color. Because of this, the IWC detection limit as well as the uncertainty of IWC improves with decreasing temperature. Regarding the difference between E_{max} = 10 and 50 (left and ~~rights~~ right panels of Figure 3) it becomes visible that the higher E_{max}, the smaller the ~~IWCs~~ IWC that can be detected.

The range of IWCs that can be detected with a H_2O_{tot} instrument can be seen from Figure 3. The blue H_2O_{enh} isolines through the IWC-T parameter space correspond to the detection limit of an instrument, e.g. the '1ppmv' and '3ppmv' H_2O_{enh} isolines represent the IWC detection limit of the FISH and HAI instruments that will be described in Section 4.1.2. Further, the IWC detection range is limited at the lower end of IWC in dependence of temperature by the requirement that H_2O_{enh}/H_2O_{gas}

> 1.05. A difference of 5% between the two measurements is necessary to avoid that artificial clouds emerge caused by the scatter of the instruments (see also Schiller et al., 2008).

3.2 IWC from cloud spectrometers

Cloud spectrometers measure the cloud particle number size distribution $\mathrm{PSD_{ice}}$. They are in most cases mounted below the the aircraft wings with sufficient distance to the wing and the aircraft body to minimize particle losses or enrichment due to distorted cloud particle trajectories or contamination by cloud particles bounced from the air frame (Krämer et al., 2013). In any case, deviations of streamlines does not play a great role in the flow around wings for particle measurements. To avoid uncertainties in the measurements caused by the aircraft's angle of attack, the cloud probes should be mounted under this angle to compensate this effect. Ice crystal shattering into small ~~artifacts~~ fragments at the cloud probes head is a source of error in $\mathrm{PSD_{ice}}$. However, it does not play a significant role for the calculation of the IWC, ~~the uncertainty from shattering does not play a significant role since the shattered crystals still~~ since the ice fragments contribute to the integrated mass of $\mathrm{PSD_{ice}}$ in the same way as the original large crystal. In addition, newer cloud spectrometers are designed in order to minimize shattering, and anti-shatter algorithms can account ice fragments stemming from large shattered ice crystals (Korolev et al., 2011). Other measurement issues of $\mathrm{PSD_{ice}}$ are discussed in detail in (Krämer et al., 2013) and Baumgardner et al. (2017).

The IWC is derived from $\mathrm{PSD_{ice}}$ by summing up the ice crystal concentrations measured in each size bin of the number size distribution. The largest source of error in this method is the irregularity of the ice crystal shapes. Especially large ice crystals cannot be assumed as spheres and their shapes strongly vary. Numerous so-called mass-dimension (m–D) or mass-area (m-A) relations are derived to account for this effect. A summary of m-D relations is given e.g. in Abel et al. (2014) and a new, advanced relation is developed by Erfani and Mitchell (2016). The m–D relations are of the form:

$$\mathrm{m_i} = \mathrm{a} \cdot \mathrm{D_i^b} \tag{3}$$

with m_i,D_i mass and diameter of the ice crystals of the i-th size bin and a, b constants of respective relations. The IWC is then:

$$\mathrm{IWC} = \sum_{\mathrm{i}=1}^{\mathrm{n}} \mathrm{m_i} \cdot \mathrm{dN_i} \tag{4}$$

4 IWC instrumentation

4.1 Bulk IWC inlet and hygrometers

4.1.1 $\mathbf{H_2O_{tot}}$ inlets

For the HALO aircraft, Trace Gas Inlets (TGI) are designed[1], mainly to probe atmospheric gas components, but also to sample ice cloud particles. The design can be seen in the bottom panel of Figure 4, where a TGI is mounted with three inlets facing

[1] *enviscope* GmbH.

in forward direction for cloud sampling and one inlet in backward direction for gas constituents. The height of the TGI and the distances of the inlets from the fuselage are designed to protrude from the aircraft's boundary layer, the numbers are listed in Table 1. The TGI inlet is heated, and the sampling tubes have a 90° bend as required to evaporate ice crystals entering the forward facing ducts (see Section 3.1.) During ML-CIRRUS in 2014, two TGIs were mounted on the frontmost apertures of HALO's roof. The roof position was chosen for the various apertures due to technical restrictions. Two H_2O_{tot} hygrometers (FISH and Waran, for description of the H_2O instruments see next section) are positioned at the upper forward inlet tips of TGI 1 and 2, a third hygrometer (HAI) is connected to the middle forward duct of the TGI 1. The TGI position at the aircraft fuselage is shown in the top panel of Figure 4. The hygrometer used for H_2O_{gas} sampling (SHARC) is connected to a backward inlet tip of a TGI mounted ~~above the wings.~~ further downstream.

On board of Geophysica, the inlet for the H_2O_{tot} hygrometer FISH is mounted at the side of the aircraft, as can be seen in Figure 5. It is also heated and has a 90° bend. The H_2O_{gas} hygrometer FLASH is mounted below a wing and equipped with it's own inlet. The WB-57 H_2O_{tot} inlet for the FISH hygrometer is mounted at the aircraft's bottom (see Figure 6) and is as well heated and has a 90° bend. The H_2O_{gas} hygrometer HWV is mounted below a wing and equipped with it's own inlet. The IWCs derived from the H_2O_{tot} measurements behind the respective inlets are here referred to as roof, side and bottom IWCs.

4.1.2 H_2O instruments

The essentials of the hygrometers used to measure H_2O_{tot} and H_2O_{gas} on board of HALO during ML-CIRRUS 2014 (FISH, HAI, Waran and SHARC) are summarized in the following. For more detail we refer to the respective cited publications of the instruments.

FISH (Fast In situ Stratospheric Hygrometer) is a closed path Lyman-α photofragment fluorescence (Zöger et al., 1999; Meyer et al., 2015) to measure H_2O_{tot} in the range of 1- 1000 ppmv between 50-500 hPa with an accuracy/precision of 6–8%/0.3 ppmv. Connected to the HALO-TGI forward facing duct, the enhancement factor range is 12-20. In accordance to Figure 3, the resulting minimum detectable IWC is between about 1-20$\cdot 10^{-3}$ ppmv ($\sim$ 1-20$\cdot 10^{-4}$ mg/m^3). The time resolution of the measurements is 1 Hz.

HAI (Hygrometer for Atmospheric Investigation) is a four channel Tunable Diode Laser hygrometer (Buchholz et al., 2017). Here, we use its closed path 1.4 µm H_2O_{tot} channel, for brevity called HAI in the following. The measurement range is 3 - 40000 ppmv with an accuracy/precision of 4.3%$\pm$3 ppmv/0.24 ppmv. Its enhancement factor at the HALO-TGI is 17-50, the resulting minimum IWC following Figure 3 is between about 0.5-20$\cdot 10^{-2}$ ppmv ($\sim$ 0.5-20$\cdot 10^{-3}$ mg/m^3) and the time resolution is 1 Hz.

Waran (Water Vapor Analyzer) is a tunable diode laser hygrometer (1.4 µm) WVSS (Vance et al., 2015), attached to the forward facing TGI (Voigt et al., 2017) instead of the originally associated inlet. The detection range is $\gtrsim$50–40000 ppmv, the accuracy according to the manufacturer is $\pm$50 ppmv or 5% of reading, whatever is larger. However, good performance of WVSS down to about 20 ppmv is reported in Smit et al. (2013) in a comparison of airborne hygrometers. The enhancement factor at the HALO-TGI is in the range of 20-35 and the resulting minimum detectable IWC is (see Figure 3) between about 0.5-50$\cdot 10^{-1}$ ppmv (0.5-50$\cdot 10^{-2}$ mg/m^3) at a time resolution of 0.4 Hz.

SHARC (Sophisticated Hygrometer for Atmospheric Research) is also a closed path Tunable Diode Laser hygrometer (1.4 µm), but at HALO used for H_2O_{gas} measurements (Meyer et al., 2015). Its range of detection is 20-40000 ppmv with an accuracy/precision of 2-4%/0.2 ppmv at a time resolution of 1 Hz.

On board of Geophysica during StratoClim 2017, H_2O_{tot} was measured by FISH, while for H_2O_{gas} FLASH (FLuorescent Airborne Stratospheric Hygrometer, for details see Khaykin et al., 2013) was used. FLASH uses also the Lyman-α photofragment fluorescence technique for the detection of water vapor, but its inlet is designed to sample only the gas phase. The detetction range is 1-1000 ppmv with an accuracy/precision of <9%/0.5 ppmv, the time resolution is 1 Hz.

FISH was also used for H_2O_{tot} measurements on board of the WB-57 during MacPex 2011. In this case, H_2O_{gas} is detected by the Lyman-α fluorescence hygrometer HWV (Harvard Water Vapor, time resolution of 1 Hz). Details of the water measurements during MacPex are described in Rollins et al. (2014).

4.2 Cloud spectrometers for IWC

During ML-CIRRUS 2014 and also StratoClim 2017, the NIXE-CAPS (New Ice eXpEriment: Cloud and Aerosol Particle Spectrometer, NIXE hereafter) instrument, mounted under the wing of HALO (see Figure 7) and Geophysica, respectively, was used to measure the cloud particle number size distribution in the size range of 3-930 µm diameter ~~(Meyer, 2012)~~at a time resolution of 1 Hz (Meyer, 2012). The mounting positions are listed in Table 1. Two instruments are incorporated in NIXE: the NIXE-CAS-DPOL (Cloud and Aerosol Spectrometer with Detection of POLarization) and the NIXE-CIPg (Cloud Imaging Probe - Greyscale). In combination, particles with diameters between 0.61 µm and 937 µm can be sized and counted. For cloud measurements, particle diameters $>$ 3 µm are considered. The data analysis methods and all applied correction algorithms are described in Meyer (2012) and Luebke et al. (2016). The IWC was derived using the m-D relation described by Krämer et al. (2016) and Luebke et al. (2016). This relation, originally derived from observations by Mitchell et al. (2010) and confirmed in the study of Erfani and Mitchell (2016), has nearly no dependency on temperature or cirrus type, thus demonstrating the robustness of the connection between cirrus ice crystal size and mass. ~~In Section 5.1.3, the~~ The m-D relation is again confirmed by ~~measurements (see also~~ our measurements, which can be seen by the good agreement of IWCs derived from PSDs from NIXE-CAPS with those determined from total water measurements with FISH (see Figure 11, left panel). A further note is that the IWCs derived from PSDs seems not to be very sensitive on the choice of the m-D relation, what can be seen in Figure 8, where, in addition to the above mentioned m-D relations, the also common m-D relations of Heymsfield et al. (2010) and Cotton et al. (2013) are plotted.

During MacPex 2011, the cloud spectrometer 2D-S (Lawson et al., 2006) was mounted under ~~the wing~~ a wingpod of the WB-57 to measure cloud particles at a time resolution of 1 Hz. The mounting position is listed in Table 1). 2D-S is an optical imaging cloud probe comparable to the CIPg, covering the particle size range of 15-1280 µm diameter. The IWC is derived from an a-D (area-dimension) relation described by Baker and Lawson (2006) which is again confirmed here (see Section 5.1.3 and Figure 11, right panel).

The IWCs derived from the wing mounted NIXE or 2D-S ice particle measurements are here referred to as ‘Wing IWCs’.

5 Ice particle probing position and IWC

5.1 IWCs from roof/side/bottom and wing sampling

5.1.1 Roof H_2O measurements

First, the measurements of the hygrometers mounted at roof of the HALO aircraft (FISH, HAI, Waran and SHARC) are compared to each other to ensure that possible instrument differences are not attributed to the probing position in the further discussion. Note here that the FISH instrument is a well-established hygrometer with a long history of successful aircraft measurements and instrument intercomparisons (Fahey et al., 2014; Rollins et al., 2014; Meyer et al., 2015). SHARC, HAI and Waran are developed for and first deployed on the HALO aircraft.

To this end, scatter plots of H_2O in clear air as well as IWCs in cirrus are shown in Figure 9. Good agreement of the clear air H_2O measurements (at $RH_{ice} < 60\%$ to strictly exclude clouds) from FISH, HAI and SHARC is demonstrated in the left panel of the figure. The middle panel show the IWC scatter plot of FISH and HAI. Most of the measurements symmetrically spread around the 1:1 line ~~by~~ within a factor of 2.5, which can be considered as a good agreement (as discussed in Section 2 and Section 5.1.4). However, the linear correlation coefficient (R^2, indicated in the panel; the correlation coefficients are given in the figure caption, the regression lines are not plotted to keep the visual clearness of the graphics) is rather low, reflecting the generally broad scatter of data points. In the right panel, the measurements of FISH and Waran are displayed. The data are mostly placed above the 1:1 line, most frequently around a factor of ~~2.~~ 2.5. This means that the IWC of Waran is shifted to higher values in comparison to FISH. An explanation for this behavior is still missing. But, R^2 is better than for HAI, i.e. the less scattered. IWCs below about 0.5 ppmv are not detected by Waran, showing the smaller IWC range of Waran (see Section 4.1.2).

5.1.2 Roof and wing IWCs

IWCs from measurements at the aircraft roof in comparison to the IWC measured under the wing are shown in Figure 10. The left/middle/right panels of the figure depict roof-mounted FISH/HAI/WARAN versus wing-mounted NIXE observations.

The first to note is the relatively broad scatter of all IWC measurements. This can be seen from the broad distribution of the data points between the black dashed lines in the panels, which represent a factor of ± 10 to the black solid 1:1 line. A closer look to the panels by taking notice of the frequencies of occurrence (see color code in the figure), however, shows narrower structures parallel to the 1:1 lines. For the FISH instrument, at medium IWCs most data pairs are placed ~~above~~ between the 1:1 ~~line~~ and 1:2.5 lines (IWC enrichment), while at higher IWCs the highest frequencies are found below the 1:10 line (IWC losses). The same is found for HAI, but at medium IWC losses are seen more often than for FISH. Vice versa, for Waran an IWC enrichment is more abundant and expands beyond the 1:2.5 line in the medium IWC range. Since no correlations between the IWC measurements can be observed here, correlation coefficients are not calculated.

5.1.3 Side/bottom and wing IWCs

To investigate if the differences of the IWCs from roof and wing measurements found in the last section might be indeed related to the H_2O_{tot} inlet position at the aircraft's roof, we analyze IWCs correlations of side/wing and bottom/wing measurements in the following.

Side IWCs were measured by FISH (H_2O_{tot}, see inlet position in Figure 5 and Table 1) together with the hygrometer FLASH for H_2O_{gas}, while wing IWCs are recorded by the cloud spectrometer NIXE during the recent field campaign StratoClim 2017 (http://www.stratoclim.org/) with the Russian aircraft Geophysica. Note here that the roof and wing ice particle measurements are performed with instruments also operated on board of HALO. Under clear sky conditions the hygrometers agree as well as those shown in Figure 9, left panel (not shown here).

A good agreement of side/wing IWCs can be seen from the left panel of Figure 11. The majority of data pairs distribute here between the thin lines, representing a factor of ± 2.5. The correlation coefficient R^2 of the linear regression is indicative for the overall scatter of data points. Since for these measurements the same instruments as for the roof/wing measurements were used for ice particle sampling, the position of the H_2O_{tot} inlet at the side of the aircraft is most probably the cause for the better agreement of the IWCs in comparison to the roof/wing IWCs discussed in the previous section (shown in Figure 10). The reason is that here the airflow clings ~~along~~ better at the aircraft fuselage because the cockpit ~~does not disturb it~~is less disturbing. Consequently, the trajectories of the ice crystals are not deflected, as it occurs at the roof of the aircraft (see Section 3). Another aspect of the good agreement between the two measurements is that it shows the validity of the m-D relation used to calculate the IWC from the PSD_{ice} measured by NIXE.

Bottom and wing IWCs were measured by FISH for H_2O_{tot} (see ~~see~~ inlet position in Figure 6; note that FISH is also deployed at HALO and Geophysica) and the hygrometer HWV for H_2O_{gas}, ~~together with~~ complemented by the cloud spectrometer 2D-S~~, mounted at~~ . The instruments are mounted on the US aircraft WB-57 during the field campaign MacPex 2011 (see Krämer et al., 2016). FISH and HWV agreed ~~also~~ well under clear sky conditions ~~, as demonstrated in Figure 9, left panel~~(not shown here).

It can be seen from Figure 11, right panel, that - beside that mostly high IWCs are found in the probed mesoscale convective cloud systems - the bottom/wing data pairs are also evenly distributed ~~around~~ between the 1:1 ~~line~~ and 1:$\pm$2.5 lines as for the side/wing observations. This is again attributed to the position of the H_2O_{tot} inlet at the bottom of the aircraft where the ice crystals are not deflected. The correlation coefficient R^2 of the linear regression is slightly better than for the side/wing measurements at Geophysica.

~~In both cases , side and bottom~~

5.1.4 Scatter of IWC measurements

In all cases of reasonable agreement between IWC measurements, in the sense of the possible agreement between IWC measurements from different ice particle sampling ~~position, the~~ positions discussed in Section 2, the IWC data distributes around the 1:1 line mostly in between a factor of ± 2.5 or better (see Figure 9: roof/roof, and Figure 11: side/wing and bottom/wing), represented by the thin lines in the Figures. This is in good agreement with a study of de Reus et al. (2009), where IWCs from H_2O_{tot} (FISH and FLASH) and cloud spectrometers (FSSP and CIP) measurements at the Russian aircraft Geophysica are compared during the field campaign SCOUT-O_3. de Reus et al. (2009) reported an IWC scatter of ± 2.2 around the 1:1 line. A scatter of IWC data in this order of magnitude is also reported by Thornberry et al. (2017), who measured IWCs by means of the side mounted NOAA-TDL hygrometer and the wing mounted cloud spectrometers FCDP and 2D-S on board of the Global Hawk during the ATTREX 2014 campaign. Abel et al. (2014) reported this quite large scatter, which in all cases exceeds the uncertainties stated for the instruments. The scatter of IWC from three instruments mounted on the WB-57 reported by Davis et al. (2007) is slightly better.

5.2 Impact of ice crystal size on roof IWC

To further investigate the structures seen in the roof/wing IWC scatter plots discussed in Section 5.1.2 (see Figure 10), we analyze the influence of the ice particle size distribution (PSD_{ice}) on the IWCs ~~. To this end~~and also ice particle trajectories of different sizes around the planes fuselage for the specific case of roof sampling considered here.

To visualize the influence of PSD_{ice} on IWC, we look at the ratio of the roof to the wing IWCs in dependence of the mean mass radius R_{ice} of the PSD_{ice} ($R_{ice} = \cancel{IWC}\left(\frac{3\cdot IWC}{4\pi\rho\cdot N_{ice}}\right)^{1/3}$ with $\rho = 0.92$ g/cm^3) from NIXE, N_{ice} = total number of ice crystals with diameter > 3 µm). The results are shown in Figure 12. In case of undisturbed sampling at both positions at the aircraft, the distribution of the data points should be homogeneous around the 1-line of the IWC-ratio, with the highest frequencies closest to this line. However, the data distribution are more 'duck' shaped for all three roof-mounted H_2O_{tot} instruments. The appearance of the IWC ratios can be divided in three regimes, marked by the thin vertical red lines in Figure 12.

(1) An IWC 'enrichment regime' is observed for small R_{ice} (about < 12 µm). A mass size distribution typical for this regime is displayed in Figure 13 (PSD_{ice} 1, top panel; note that for the portrayal of the ~~PSD we~~ PSDs we here use the ice particle diameter and not radius to clearly distinguish from the mean mass radius R_{ice} of the ice particle population used in Figures 12). The ice mass of PSD_{ice} 1 accumulates at smaller sizes, larger ice particles does not contribute to the IWC. Following Section 3 (Figure 1), smaller ice crystals at the aircraft roof are enriched close to the fuselage and this is what Figure 12 ~~demonstrates. Further, this is consistent~~ shows, in consistency with the enrichment at lower IWC seen in Figure 10.

Supportive to this finding based on the experimental approach of comparative IWC measurements, we performed three-dimensional CFD calculations of gas streamlines and ice particle trajectories around an aircraft with a HALO-type fuselage, shown in Figure 14. In panel (a) trajectories of ice crystals as small as 5 µm diameter are plotted (thick lines). It can be seen from the Figure that the gas streamlines (thin lines, color coded by the velocity of the flow) are compressed, in accordance with the potential flow calculations. Consequently, the probed air volume is compressed for smaller ice crystals which follow the streamlines, which leads to the observed enrichment of IWC.

(2) An IWC ‘loss regime’ is detected in Figure 12 for large mean mass R_{ice} (about $\gtrsim$ 25 µm). Here, the IWC originates mainly from large ice crystals connected to PSD_{ice} 3 in Figure 13 that are not sampled in the shadow zone at the aircraft roof. A shadow zone can also be seen in the CFD simulation in Figure 14, panels (b) and (c). Ice particles of 50 and 100 µm miss the inlet or hit the plane, respectively. Note that the width of the shadow zone differ for the different particle sizes, it increases for the 100 µm ice particles in comparison to those with 50 µm. However, also some cases of IWC oversampling (IWC ratios > 1 in Figures 12) are found for large ice crystals. This might be explained by cases where huge ice crystals are present, which meet the inlet directly, as can be seen in panel (d) of Figure 14 (500 µm particle trajectory), but come from air outside of the original sampling volume.

(3) An IWC ‘even-handed regime’ is found (Figure 12) for intermediate R_{ice} (about 12-25 µm). The corresponding typical PSD_{ice} 2 can be seen in the middle panel of Figure 13. This type of PSD_{ice} is bimodal with one ice mass peak at smaller and another at larger sizes. Depending on which of the peaks is dominating, the accumulation of smaller ice crystals in the aircraft’s enrichment zone or the losses of larger ice crystals in the shadow zone overbalance.

~~(3) A ‘loss regime’ is detected for large (about $\gtrsim$ 25 m). Here, the large ice crystals connected to PSD_{ice} 3 shown in Figure 13are not sampled in the shadow zone at the aircraft roof. The losses of roof IWC at higher IWCs shown in Figure 10correspond to this regime.~~

The ’duck’ shape of the IWC ratios of the three instruments slightly differ from each other. Most equally distributed around the ratio 1 are the FISH/NIXE IWCs (top panel of Figure 12), with the highest frequencies in the enrichment part of the ‘even-handed regime’ at IWC ratios slightly above 1. HAI/NIXE IWC ratios (middle panel of Figure 12) on the other hand have the highest frequencies in the loss part of the ‘even-handed regime’ reaching IWC ratios significantly below 1. This is consistent with the fact that the HAI instrument is connected to the middle forward inlet (see Figure 4) and is thus -in comparison to the FISH inlet- closer to the fuselage. Here, the losses of large particles are more pronounced. Notable is that already a few centimeter have such a large effect on the particle sampling efficiency. The bottom panel of Figure 12 shows the Waran/NIXE IWC ratios. Waran is connected -as FISH- to the roof inlet of a TGI right next to that of FISH and thus shows a comparable distribution of frequencies, but shifted to higher values. This reflects that the Waran IWCs are in general somewhat higher than those of the other instruments (see Figures 9 and 10).

5.3 Roof and wing IWC climatologies

An overview of the impact of the sampling position on the IWC is given in Figures 15, where IWC frequencies of occurrence are shown in dependence of temperature for the roof-mounted FISH instrument (top panel) and the wing-mounted NIXE (bottom panel).

Comparing the roof and wing IWCs at warmer temperatures, it can be clearly seen that high IWCs are not measured at the roof position and thus the higher frequencies are shifted to lower IWCs. The reason is most probably that high IWCs at temperatures $\gtrsim$ 220 K are related to large ice crystal sizes belonging to the ’loss regime’ discussed in the previous section, which can be seen in Figures 15 (bottom panel), where frequencies of occurrence of R_{ice} in dependence of temperature are plotted. At lower temperatures, the mean mass ice crystal sizes R_{ice} shrinks into the 'even-handed' and 'enrichment regime' that means they are often enriched, resulting in an overestimation of the roof IWCs. This can be seen in the higher frequencies of larger roof IWCS in comparison to the wing IWCs.

Altogether, the IWC climatology of the roof IWCs covers roughly the same range as that of the wing IWCs, with the exception that large IWCs at high temperatures are missed. However, the distribution of the frequencies of occurrence of the IWCs is, caused by the position of the H_2O_{tot} inlet, heavily skewed for the roof IWCs.

6 Summary and conclusions

~~IWC is measured at three positions of aircraft fuselages,~~ The influence of the ice particle sampling position on IWC measurements on aircraft is investiagted with the approach of comparative measurements. The reproducibility of the underlying total water measurements is assessed comparison with several instruments at the same position as well as with as phase water instruments. The representativeness of the corresponding IWC measurements at roof, side and bottom ~~, as well as under the wing. The~~ mountings on the fuselage is evaluated by comparison with IWCs derived from ice particle size distributions measured under the aircraft wing.

The side and bottom IWC in comparison to wing IWC measurements show a ~~satisfactory good agreementbetween side/bottom and wing IWCs, most~~ reasonable good agreement. Most frequently they correspond to each other within a factor of 2.5, independently of the mean ice crystal sizes. ~~This is because~~ The reason for the only little disturbed measurements at these positions is that under the aircraft wing and at the side and bottom of the fuselage, the ~~cirrus~~ cloud particle trajectories are not greatly diverted caused by the aircraft body or the wing itself, so that the sampling of ice crystals represent nearly ambient conditions.

~~In addition~~But, the agreement of the IWCs does not only show the performance of the side, bottom and wing sampling position, but also the ~~agreement of the IWC instrumentation~~credibility of the measurements. This is notable since the measurement techniques greatly differ, the side/bottom IWC is measured by the Lyman–α fluorescence hygrometer FISH and the wing IWC is obtained from the ice particle mass size distribution measured by optical methods with NIXE-CAPS and 2D-S. A further conclusion from the agreement of the IWCs is that it demonstrates the validity of the m-D relation of Erfani and Mitchell (2016), slightly modified by Krämer et al. (2016) and Luebke et al. (2016), which is applied to convert the NIXE-CAPS size of the ice crystals into mass.

However, roof and wing IWCs differ from each other. ~~The reason is that the cockpit causes deviations~~ Since from the side and bottom in comparison to wing measurements the instrument performance is shown, we attribute the differences to the mounting position on the roof. Deviations of the streamlines and particle ~~trjectories~~ trajectories above the roof ~~, leading~~ due to the cockpit can lead to both, enrichment and losses of particles depending on the size of the ice particles. Large ice particles are lost in the shadow-zone behind the aircraft's cockpit, while at the same time smaller ice crystals are enriched. ~~For~~ These -expected- findings from the approach of comparative measurements are supported by CFD simulations performed for different ice particle sizes. A more detailed analysis shows that for the measuremets performed in this study the mean mass radii of the ice particle population smaller than about 12 µm~~(range 2 - 100 m)~~, enrichment of the ice crystals and thus an overestimation of the IWC dominates. In the size range 12 to about 25 µm both enrichment and losses of ice crystal occurs, while loss of large crystals leading to strongly underestimated IWCs prevails for larger sizes. Enrichment and losses are in the order of a factor of 10 or more.

A correction of the IWCs measured at aircraft roofs might only be possible when ice particle PSDs are measured simultaneously. However, in that case the IWCs calculated from the PSDs would still be more accurate. Because of the high variability of the ice particle size distributions, it is also not an option to assume PSDs, e.g. in dependence of temperature, for a correction of the roof IWCs.

The influence of the size dependent enrichment or losses of ice crystals from the roof sampling propagates to IWC climatologies with respect to temperatures. At higher temperatures, where the ice crystals are larger, IWCs are underestimated due to the ice particle losses, while at lower temperatures overestimation of IWC caused by particle enrichment dominates.

The recommendations resulting from this comparison of in-situ measurements of IWC are that (i) reliable measurements of IWC are possible from sampling positions at the side, bottom and under the wing when using (ii) instruments with a detection range that cover the complete wide IWC range from about 0.001 to 3000 ppmv, and (iii) placing the instruments far enough away from the fuselage to minimize possible effects of flow distortions. The best approach to measure IWC is to deploy a combination of two instruments at different sampling positions. As last remark we like to note that this recommendations also applies to other ice particle measurements, such as ice crystal numbers sampled by counterflow virtual impactors (Mertes et al., 2007).

Author contributions.

A. Afchine: NIXE-CAPS measurements and IWC analysis; M. Krämer: FISH and NIXE-CAPS measurements, IWC analysis; C. Rolf: FISH measurements and IWC analysis; A. Costa: NIXE-CAPS measurements; N. Spelten: FISH measurements; M. Riese: FISH and NIXE deployment; B. Buchholz: HAI measurements; V. Ebert: HAI measurements; R. Heller: Waran measurements; S. Kaufmann: Waran measurements; C. Voigt: Waran measurements; M. Zöger: SHARC measurements; P. Lawson: 2D-S measurements; J. Smith: HWV measurements; A. Lykov: FLASH measurements; S. Khaykin: FLASH measurements ; A. Minikin: under wing cloud spectrometer configuration.

Acknowledgements. The authors would like to thank the DFG (Deutsche Forschungsgemeinschaft, German Research Foundation) Priority Program SPP 1294 for funding of the FZJ project 'ACIS' (KR 2957/1-1) and the PTB HAI project (EB 235/3-1 and EB 235/3-2). C. Voigt thanks for finding by HGF contract No. W2/W3-60 and by DFG SPP HALO 1294 contract No. V01504/4-1. Special thanks to our colleagues S. Mertes (TROPOS, Leipzig) and H. Ziereis (DLR, Wessling) for stimulating and important discussions on the topic of ice crystal sampling from aircraft roof.

References

Abel, S. J., Cotton, R. J., Barrett, P. A., and Vance, A. K.: A comparison of ice water content measurement techniques on the FAAM BAe-146 aircraft, Atmospheric Measurement Techniques, 7, 3007–3022, https://doi.org/10.5194/amt-7-3007-2014, https://www.atmos-meas-tech.net/7/3007/2014/, 2014.

Baker, B. and Lawson, R. P.: Improvement in determination of ice water content from two-dimensional particle imagery. Part I: Image-to-mass relationships, JOURNAL OF APPLIED METEOROLOGY AND CLIMATOLOGY, 45, 1282–1290, https://doi.org/10.1175/JAM2398.1, 2006.

Baumgardner, D., Abel, S. J., Axisa, D., Cotton, R., Crosier, J., Field, P., Gurganus, C., Heymsfield, A., Korolev, A., Krämer, M., Lawson, P., McFarquhar, G., Ulanowski, Z., and Um, J.: Cloud Ice Properties: In Situ Measurement Challenges; Chapter 9 of 'Ice Formation and Evolution in Clouds and Precipitation: Measurement and Modeling Challenges', Meteorol. Monographs, https://doi.org/10.1175/AMSMONOGRAPHS-D-16-0011.1, 2017.

Buchholz, B., Afchine, A., Klein, A., Schiller, C., Krämer, M., and Ebert, V.: HAI, a new airborne, absolute, twin dual-channel, multi-phase TDLAS-hygrometer: background, design, setup, and first flight data, ATMOSPHERIC MEASUREMENT TECHNIQUES, 10, 35–57, https://doi.org/10.5194/amt-10-35-2017, 2017.

Cotton, R. J., Field, P. R., Ulanowski, Z., Kaye, P. H., Hirst, E., Greenaway, R. S., Crawford, I., Crosier, J., and Dorsey, J.: The effective density of small ice particles obtained from in situ aircraft observations of mid-latitude cirrus, Quarterly Journal of the Royal Meteorological Society, 139, 1923–1934, https://doi.org/10.1002/qj.2058, 2013.

Davis, S. M., Avallone, L. M., Weinstock, E. M., Twohy, C. H., Smith, J. B., and Kok, G. L.: Comparisons of in situ measurements of cirrus cloud ice water content, J. Geophys. Res., 112, https://doi.org/10.1029/2006JD008214, 2007.

de Reus, M., Borrmann, S., Bansemer, A., Heymsfield, A., Weigel, R., Schiller, C., Mitev, V., Frey, W., Kunkel, D., Kürten, A., Curtius, J., Sitnikov, N., Ulanovsky, A., and Ravegnani, F.: Evidence for ice particles in the tropical stratosphere from in-situ measurements, Atmos. Chem. Phys., 9, 67756792, 2009.

Erfani, E. and Mitchell, D. L.: Developing and bounding ice particle mass- and area-dimension expressions for use in atmospheric models and remote sensing, Atmospheric Chemistry and Physics, 16, 4379–4400, https://doi.org/10.5194/acp-16-4379-2016, https://www.atmos-chem-phys.net/16/4379/2016/, 2016.

Fahey, D., Gao, R., Möhler, O., Saathoff, H., Schiller, C., Ebert, V., Krämer, M., Peter, T., Amarouche, N., Avallone, L. M., Bauer, R., Bozóki, Z., Christensen, L. E., Davis, S. M., Durry, G., Dyroff, C., Herman, R. L., Hunsmann, S., Khaykin, S. M., Mackrodt, P., Meyer, J., Smith, J. B., Spelten, N., Troy, R. F., Vömel, H., Wagner, S., and Wienhold, F. G.: The AquaVIT-1 intercomparison of atmospheric water vapor measurement techniques, AMT, 7, 3177–3213, https://doi.org/doi:10.5194/amtd-7-3177-2014, 2014.

Gayet, J.-F., Ovarlez, J., Shcherbakov, V., Ström, M., Schumann, U., Minikin, A., Auriol, F., Petzold, A., and Monier, M.: Cirrus cloud microphysical and optical properties at southern and northern midlatitudes during the INCA experiment, J. Geophys. Res., 109, D20206, https://doi.org/10.1029/2004JD004803, 2004.

Heymsfield, A. J., Winker, D., Avery, M., Vaughan, M., Diskin, D., Deng, M., Mitev, V., and Matthey, R.: Relationships between ice water content and volume extinction coefficient from in situ observations for temperatures from 0° to 86°C: Implications for spaceborne lidar, J. Appl. Meteorol. Climatol., 53, 479–505, https://doi.org/10.1175/JAMC-D-13-087.1, 2014.

Heymsfield, A. J., Schmitt, C., Bansemer, A., and Twohy, C. H.: Improved Representation of Ice Particle Masses Based on Observations in Natural Clouds, Journal of the Atmospheric Sciences, 67, 3303–3318, https://doi.org/10.1175/2010JAS3507.1, 2010.

Khaykin, S. M., Engel, I., Vömel, H., Formanyuk, I. M., Kivi, R., Korshunov, L. I., Krämer, M., Lykov, A. D., Meier, S., Naebert, T., Pitts, M. C., Santee, M. L., Spelten, N., Wienhold, F. G., Yushkov, V. A., , and Peter, T.: Arctic stratospheric dehydration – Part 1: Unprecedented observation of vertical redistribution of water, Atmos. Chem. Phys., 13, 11 503 – 11 517, https://doi.org/10.5194/acp-13-11503-2013, 2013.

King, W. D.: Air flow and particle trajectories around aircraft fuselages I: Theory, J. Atmos. Ocean. Techn., 1, 5–13, 1984.

Korolev, A., Emery, E., Strapp, J., Cober, S., Isaac, G., Wasey, M., and Marcotte, D.: Small ice particles in tropospheric clouds: fact or artifact? Airborne Icing Instrumentation Evaluation Experiment, Bull. Am. Meteorol. Soc., 92, 967–973, https://doi.org/10.1175/2010BAMS3141.1, 2011.

Krämer, M. and Afchine, A.: Sampling characteristics of inlets operated at low U/U0 ratios: new insights from computational fluid dynamics (CFX) modeling, J. Aerosol Sci., 35, 683 – 694, 2004.

Krämer, M., Rolf, C., Luebke, A., Afchine, A., Spelten, N., Costa, A., Meyer, J., Zoeger, M., Smith, J., Herman, R. L., Buchholz, B., Ebert, V., Baumgardner, D., Borrmann, S., Klingebiel, M., and Avallone, L.: A microphysics guide to cirrus clouds - Part 1: Cirrus types, Atmospheric Chemistry and Physics, 16, 3463–3483, https://doi.org/10.5194/acp-16-3463-2016, 2016.

Krämer, M., Twohy, C., Hermann, M., Afchine, A., Dhaniyala, S., Korolev, A.; Eds. Wendisch, M., and Brenguier, J.-L.: Aerosol and Cloud Particle Sampling, In: Airborne Measurements for Environmental Research: Methods and Instruments, Ed. Wendisch, M. and Brenguier, J.-L., Wiley-VCH Verlag GmbH & Co. KGaA, https://doi.org/10.1002/9783527653218.ch6, 2013.

Lawson, R., O'Connor, D., Zmarzly, P., Weaver, K., Baker, B., Mo, Q., and Jonsson, H.: The 2D – S (Stereo) probe: Design and preliminary tests of a new airborne, high – speed, high – resolution particle Imaging probe, J. Atmos. Ocean. Technol., 23, 1462 – 1477, 2006.

Luebke, A., Avallone, L., Schiller, C., Meyer, J., Rolf, C., and Krämer, M.: Ice water content of Arctic, midlatitude, and tropical cirrus – Part 2: Extension of the database and new statistical analysis, ACP, 13, 6447–6459, 2013.

Luebke, A. E., Afchine, A., Costa, A., Grooss, J.-U., Meyer, J., Rolf, C., Spelten, N., Avallone, L. M., Baumgardner, D., and Krämer, M.: The origin of midlatitude ice clouds and the resulting influence on their microphysical properties, Atmospheric Chemistry and Physics, 16, 5793–5809, https://doi.org/10.5194/acp-16-5793-2016, 2016.

Mertes, S., Verheggen, B., Walter, S., Connolly, P., Ebert, M., Schneider, J., Bower, K. N., Cozic, J., Weinbruch, S., Baltensperger, U., and Weingartner, E.: Counterflow virtual impact or based collection of small ice particles in mixed-phase clouds for the physico-chemical characterization of tropospheric ice nuclei : Sampler description and first case study, AEROSOL SCIENCE AND TECHNOLOGY, 41, 848–864, https://doi.org/10.1080/02786820701501881, 2007.

Meyer, J.: Ice Crystal Measurements with the New Particle Spectrometer NIXE-CAPS, Schriften des Forschungszentrums Jülich. Reihe Energie und Umwelt / Energy and Environment; 160; ISBN:9783893368402, 2012.

Meyer, J., Rolf, C., Schiller, C., Rohs, S., Spelten, N., Afchine, A., Zöger, M., Sitnikov, N., Thornberry, T., Rollins, A., Gao, R., Bozoki, Z., Tatrai, D., Buchholz, B., Ebert, V., Mackrodt, P., Möhler, O., Saathoff, H., Rosenlof, K., and Krämer, M.: Two decades of water vapor measurements with the FISH fluorescence hygrometer: A review., ACP, 15, 8521–8538, https://doi.org/10.5194/acp-15-8521-2015, 2015, 2015.

Mitchell, D. L., D'Entremont, R. P., and Lawson, R. P.: Inferring Cirrus Size Distributions through Satellite Remote Sensing and Microphysical Databases, Journal of the Atmospheric Sciences, 67, 1106–1125, https://doi.org/10.1175/2009JAS3150.1, 2010.

Rollins, A. W., Thornberry, T. D., Gao, R. S., Smith, J. B., Sayres, D. S., Sargent, M. R., Schiller, C., Krämer, M., Spelten, N., Hurst, D. F., Jordan, A. F., Hall, E. G., Vömel, H., Diskin, G. S., Podolske, J. R., Christensen, L. E., Rosenlof, K. H., Jensen, E. J., and Fahey,

D. W.: Evaluation of UT/LS hygrometer accuracy by intercomparison during the NASA MACPEX mission, JGR, 119, 1915–1935, https://doi.org/doi:10.1002/2013JD020817, 2014.

Schiller, C., Krämer, M., Afchine, A., Spelten, N., and Sitnikov, N.: Ice water content in Arctic, midlatitude and tropical cirrus, J. Geophys. Res., 113, D24208, https://doi.org/doi:10.1029/2008JD010342., 2008.

Smit, H., Krämer, M., Petzold, A., Rolf, C., Spelten, N., Rohs, S., Neis, P., Ebert, V., Buchholz, B., Bozoki, Z., Tatrai, D., Jones, R., Mead, M., and Malinowski, S.: Development and evaluation of novel compact hygrometers for airborne research (DENCHAR): Assessment report on the performance of the suite of hygrometers and recommendations, Eufar research report, Forschungszentrum Jülich, Jülich, Germany, 2013.

Thornberry, T., Rollins, A., Avery, M., Woods, S., Lawson, R., Bui, T., and Gao, R.-S.: Ice water content-extinction relationships and effective diameter for TTL cirrus derived from in situ measurements during ATTREX 2014, J. Geophys. Res., 122, 4494–4507, https://doi.org/10.1002/2016JD025948, 2017.

Twohy, C. and Rogers, D.: Air-flow and water-drop trajectories at instrument sampling points around the Beechcraft King Air and Lockheed Electra, Journal of Atmospheric and Oceanic Technology, 10, 566–578, https://doi.org/10.1175/1520-0426(1993)010<0566:AAWDTA>2.0.CO;2, 1993.

Vance, A. K., Abel, S. J., Cotton, R. J., and Woolley, A. M.: Performance of WVSS-II hygrometers on the FAAM research aircraft, Atmospheric Measurement Techniques, 8, 1617–1625, https://doi.org/10.5194/amt-8-1617-2015, https://www.atmos-meas-tech.net/8/1617/2015/, 2015.

Voigt, C., Schumann, U., Minikin, A., Abdelmonem, A., Afchine, A., Borrmann, S., Boettcher, M., Bucuchholz, B., Bugliaro, L., Costa, A., Curtius, J., Dollner, M., Doernbrack, A., Dreiling, V., Ebert, V., Ehrlich, A., Fix, A., Forster, L., Frank, F., Fuetterer, D., Giez, A., Graf, K., Grooss, J.-U., Gross, S., Heimerl, K., Heinold, B., Hueneke, T., Jaervinen, E., Jurkat, T., Kaufmann, S., Kenntner, M., Klingebiel, M., Klimach, T., Kohl, R., Krämer, M., Krisna, T. C., Luebke, A., Mayer, B., Mertes, S., Molleker, S., Petzold, A., Pfeilsticker, K., Port, M., Rapp, M., Reutter, P., Rolf, C., Rose, D., Sauer, D., Schaefer, A., Schlage, R., Schnaiter, M., Schneider, J., Spelten, N., Spichtinger, P., Stock, P., Walser, A., Weigel, R., Weinzierl, B., Wendisch, M., Werner, F., Wernli, H., Wirth, M., Zahn, A., Ziereis, H., and Zoger, M.: ML-Cirrus the airborne experiment on natural cirrus and contrail cirrus with the high-altitude long-range research aircraft HALO, Bulletin of the American Meteorological Society, 98, 271–288, https://doi.org/10.1175/BAMS-D-15-00213.1, 2017.

Weigel, R., Spichtinger, P., Mahnke, C., Klingebiel, M., Afchine, A., Petzold, A., Krämer, M., Costa, A., Molleker, S., Reutter, P., Szakall, M., Port, M., Grulich, L., Jurkat, T., Minikin, A., and Borrmann, S.: Thermodynamic correction of particle concentrations measured by underwing probes on fast-flying aircraft, Atmospheric Measurement Techniques, 9, 5135–5162, https://doi.org/10.5194/amt-9-5135-2016, 2016.

Wendisch, M. and Brenguier, J.-L. E.: Airborne Measurements for Environmental Research: Methods and Instruments, Wiley-VCH Verlag GmbH & Co. KGaA, ISBN:13:978-352740996, 2013.

Zöger, M., Afchine, A., Eicke, N., Gerhards, M.-T., Klein, E., McKenna, D., Mörschel, U., Schmidt, U., Tan, V., Tuitjer, F., Woyke, T., and Schiller, C.: Fast in situ stratospheric hygrometers: A new family of balloon-borne and airborne Lyman- photofragment fluorescence hygrometers., J. Geophys. Res., 104, 1807–1816, 1999.

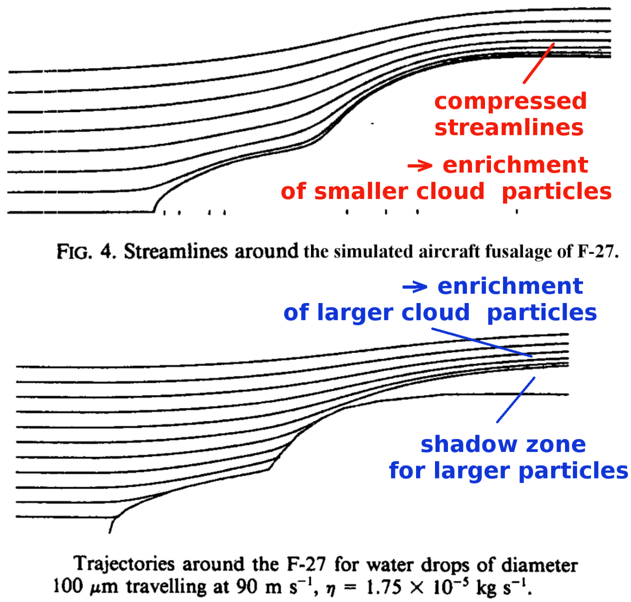

Figure 1. ~~Two-dimensional~~ Three-dimensional potential flow simulations of gas streamlines and particle trajectories around an aircraft shaped body, adapted from King (1984) (with annotations).

Figure 2. Sub-isokinetic sampling of ice particles by a nearly virtual inlet, where the velocity U inside of the inlet tube is much smaller than the flow speed U_0. The dashed lines denote the region of the free stream from where the gas streamlines enter the inlet; the black dots illustrate large particles that do not follow the gas streamlines, particle tracks are indicated by thin solid lines (adapted from Krämer et al., 2013).

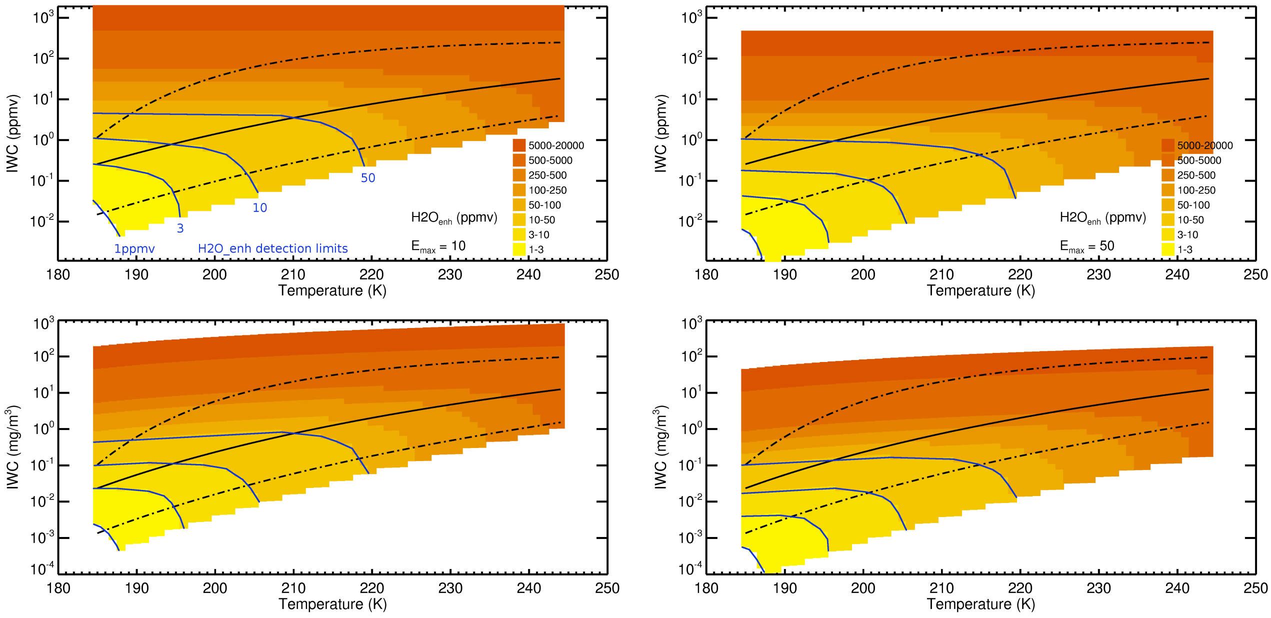

Figure 3. Relation between H_2O_{enh} and IWC in dependence of temperature for given H_2O_{gas} (assumed as water vapor saturation value), calculated from Eq. 1 ($\mathrm{IWC} = \frac{H_2O_{enh} - H_2O_{gas}}{E_{max}}$) for two different E_{max} (left: 10, right: 50); top: volume mixing ratio, bottom: concentration). The minimum difference between H_2O_{enh} and H_2O_{gas} to detect IWC is 5% to account for measurement uncertainties, i.e. in the white region below the calculated IWCs, $H_2O_{enh}/H_2O_{gas} < 1.05$. Blue lines: H_2O_{enh} isolines corresponding to the detection limit of an instrument, e.g. the '1ppmv' and '3ppmv' H_2O_{enh} isolines represent the IWC detection limit of the FISH and HAI instruments described in Section 4.1.2. Black solid and dashed lines: medium, core max and min IWCs after Schiller et al. (2008).

Figure 4. Roof mounted FISH, HAI, Waran inlet at HALO (photos: top A. Fix, bottom A. Afchine).

Figure 5. Side mounted FISH-inlet at Geophysica (photo: A. Afchine).

Figure 6. Bottom mounted FISH-inlet at WB-57 (photo: A. Afchine).

Figure 7. NIXE underwing mounting at HALO (photo: A. Afchine).

HALO (Gulfstream GV)							
Inlet (roof)						**PMS** (wing)	
FISH		HAI		Waran		NIXE-CAPS	
Distance from nose [cm]	Distance to fuselage [cm]	Distance from nose [cm]	Distance to fuselage [cm]	Distance from nose [cm]	Distance to fuselage [cm]	Distance from leading edge of the wing [cm]	Distance to wing surface [cm]
650	31.9	650	26.4	650	31.9	15	30

Geophysica (M-55)				WB-57 (NASA)			
Inlet (side)		**PMS** (wing)		**Inlet** (bottom)		**PMS** (wing)	
FISH		NIXE-CAPS		FISH		2-DS	
Distance from nose [cm]	Distance to fuselage [cm]	Distance from leading edge of the wing [cm]	Distance to wing surface [cm]	Distance from nose [cm]	Distance to fuselage [cm]	Distance from leading edge of the wingpod [cm]	Distance to wingpod surface [cm]
500	35	50	50	900	35	- 150	50

Table 1. Positions of the total water inlets and cloud spectrometers at the three aircraft (see Figures 4 - 7).

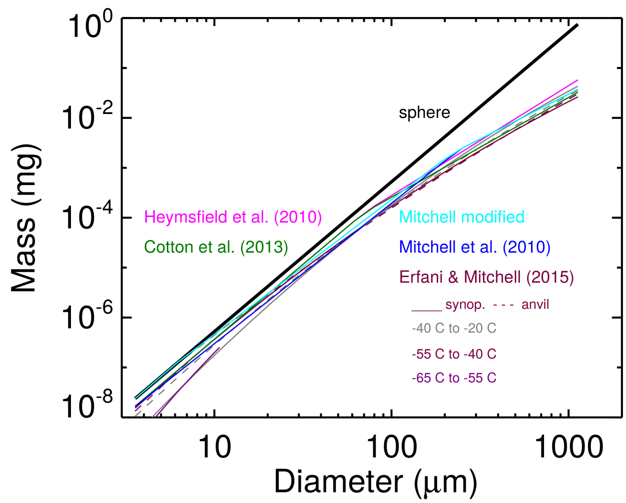

sphere
Heymsfield et al. (2010)
Cotton et al. (2013)
Mitchell modified
Mitchell et al. (2010)
Erfani & Mitchell (2015)
synop. - - - anvil
-40 C to -20 C
-55 C to -40 C
-65 C to -55 C
Mass (mg)
Diameter (μm)
10
100
1000

Figure 8.

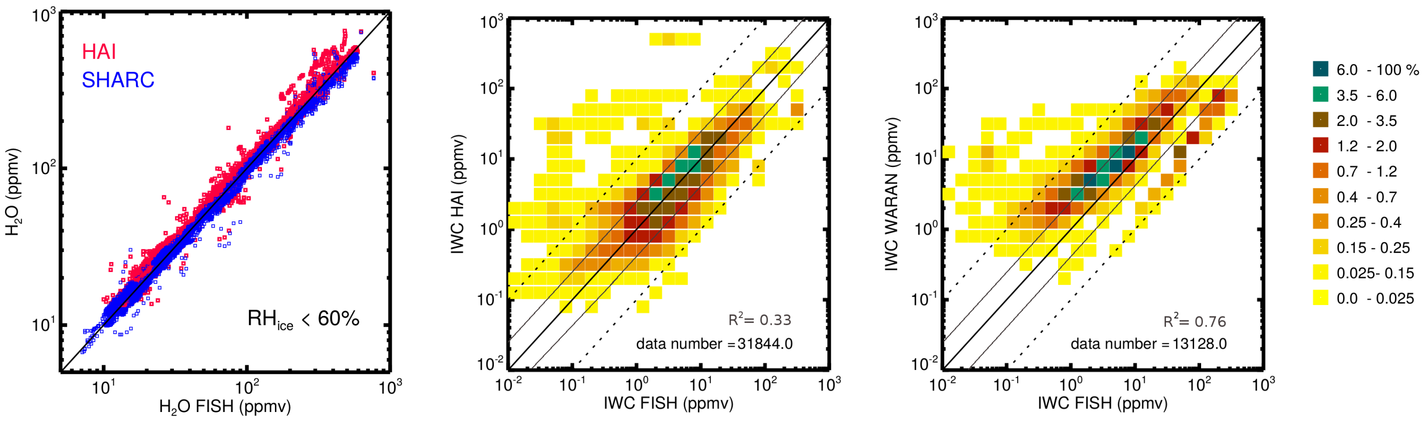

Figure 9. Comparison of H_2O and IWCs from roof-mounted closed-path hygrometers FISH~~and~~, HAI and WARAN (H_2O_{tot}) and SHARC (H_2O_{gas}) @HALO during ML-CIRRUS 2014 (color code: frequencies; solid black: 1:1 line; dashed/thin: ± factor 10/2.5 to 1:1 line). Linear regression coefficients for X=log(IWC FISH), Y=log(IWC HAI/WARAN) are: FISH/HAI (middle) Y = 0.481·X + 0.270, Stddev X = 0.534, FISH/WARAN (right) Y = 0.651·X + 0.562, Stddev X = 0.736; the coerrelation coefficients R^2 are shown in the respective panels.

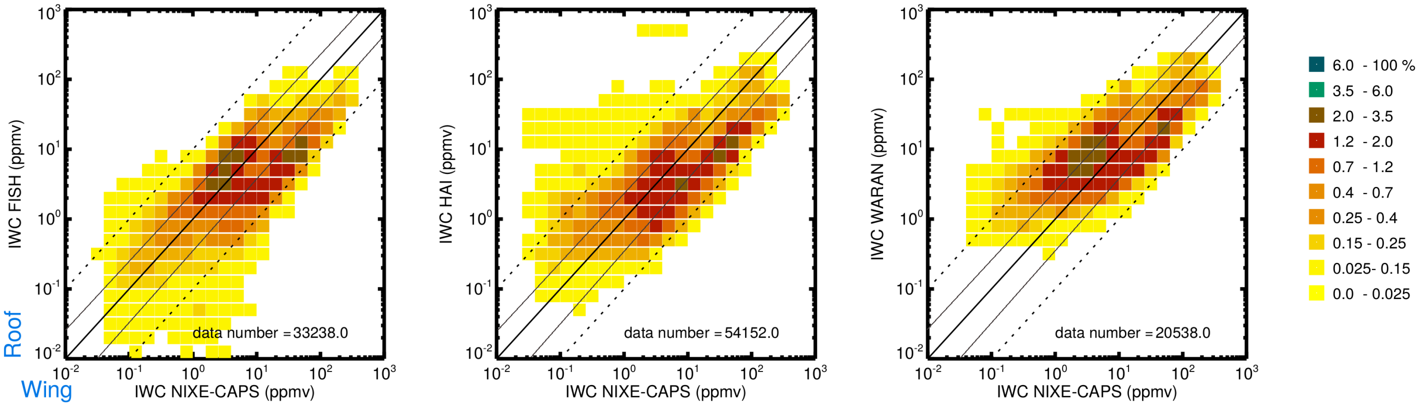

Figure 10. Comparison of IWCs from roof-mounted closed-path hygrometers FISH, HAI and Waran (see Equation 1, H_2O_{gas} from SHARC) and wing-mounted cloud spectrometer NIXE @HALO during ML-CIRRUS 2014 (color code: frequencies; solid black: 1:1 line; dashed/thin: ± factor 10/2.5 to 1:1 line).

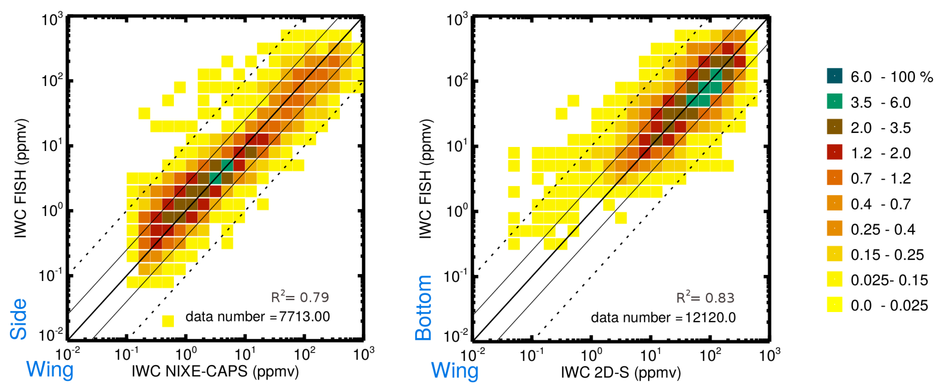

Figure 11. Comparison of IWCs from left: side mounted closed-path FISH (see Equation 1, H_2O_{gas} from FLASH) and wing-mounted cloud spectrometer NIXE @Geophysica during StratoClim 2017; right: bottom-mounted closed-path FISH (see Equation 1, H_2O_{gas} from HWV) and wing-mounted cloud spectrometer 2D-S @WB-57 during MacPex 2011 (color code: frequencies; solid black: 1:1 line; dashed/thin: ± factor 10/2.5 to 1:1 line). Linear regression coeffecients for X=log(IWC Wing), Y=log(IWC Side/Bottom) are: Side/Wing (right) Y = 0.779·X + 0.0484, Stddev X = 0.685; Bottom/Wing (right) Y = 0.856·X + 0.174, Stddev X = 0.719; the coerrelation coefficients R^2 are shown in the respective panels.

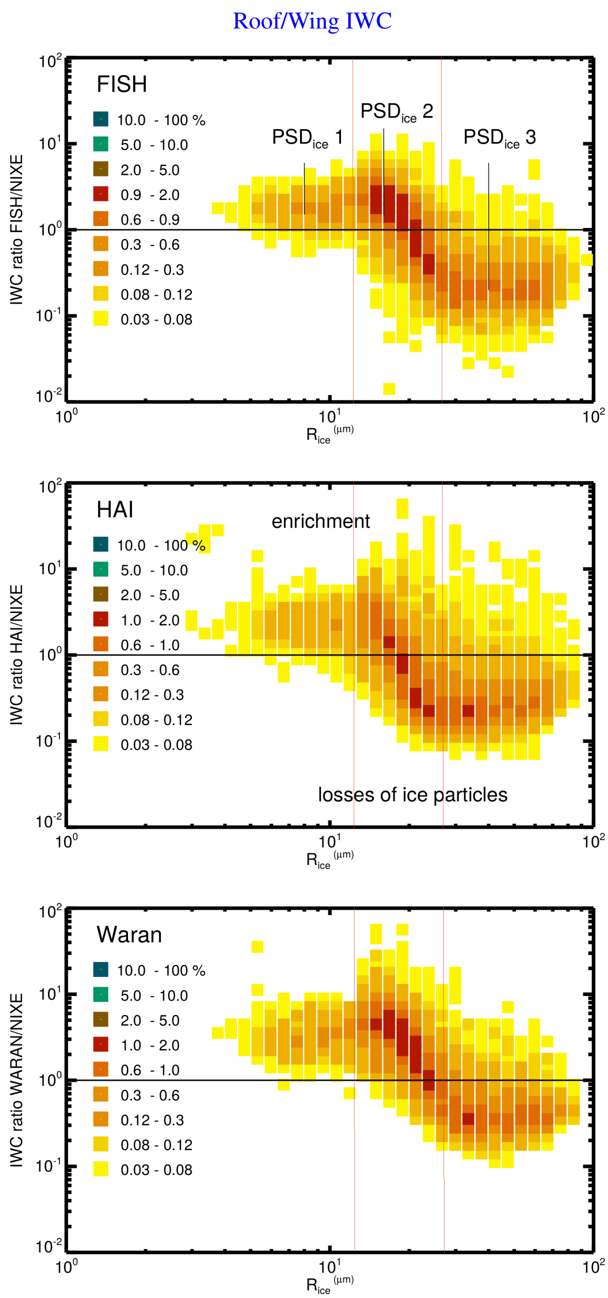

Figure 12. Ratios of Roof/Wing IWC (Roof IWC from FISH, HAI, Waran; Wing IWC from NIXE) vs. mean mass R_{ice}.

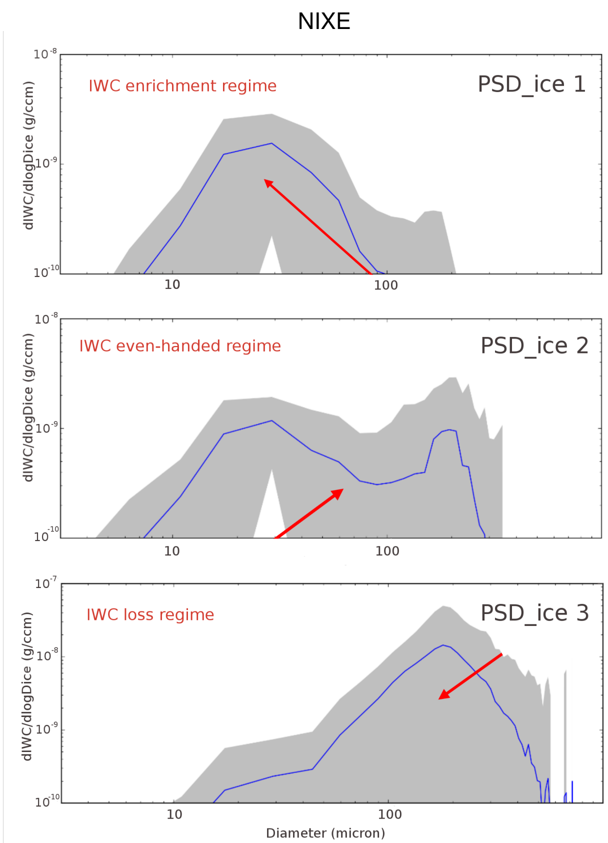

Figure 13. Three types of cirrus mass size distributions dIWC/dlogD_{ice}, exemplarily for the flight on 4. April 2014. Blue lines represent the mean PSDs, the grey area the standard deviation; note that for the portrayal of the PSD we use the ice particle diameter and not radius to clearly distinguish from the mean mass radius R_{ice} of the ice particle population used in Figures 12.

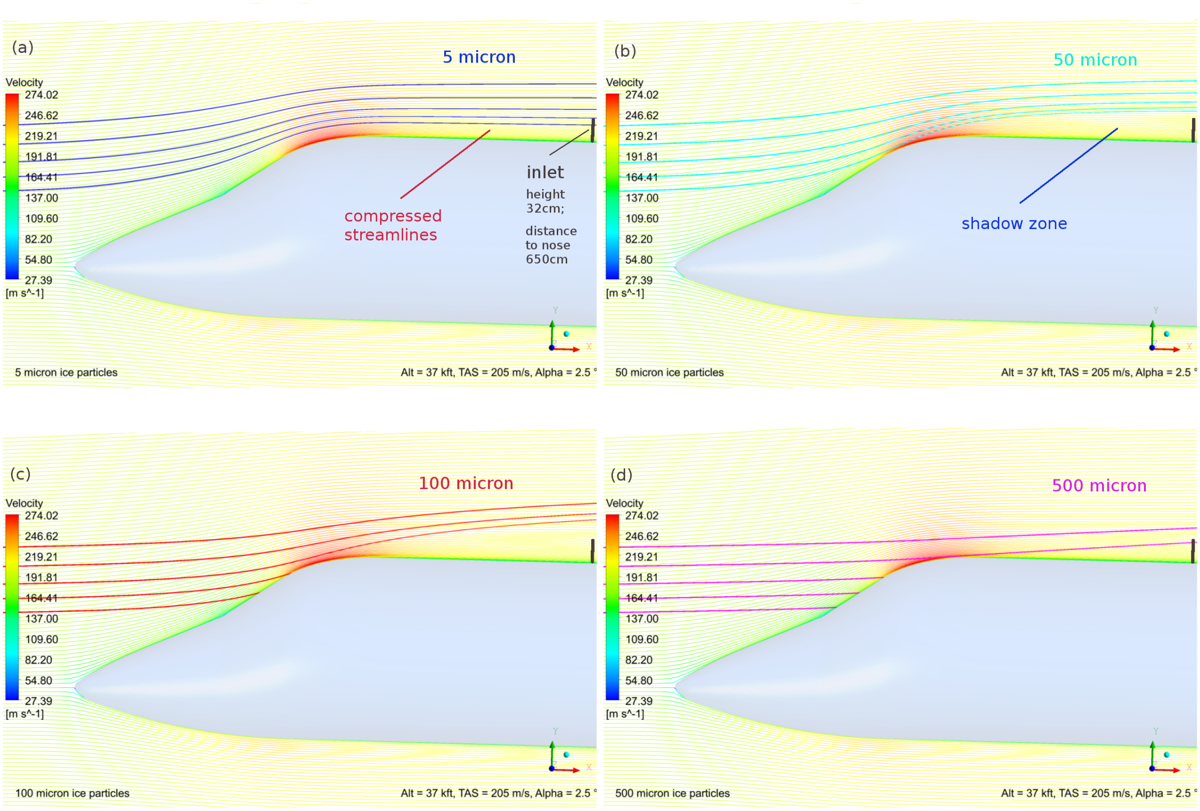

Figure 14. Two-dimensional CFD calculations of gas streamlines (thin lines, color coded by the velocity of the flow) and ice particle trajectories (thick colored lines) around an aircraft with a fuselage similar to the HALO aircraft (note that for legal reasons, the exact envelope of HALO can not be simulated). The IWC inlet is placed at the roof at the same position as the TGI on HALO (see Figure 4, Section 4.1.1). The simulations are performed for typical conditions during penetrations of cirrus clouds: Altitude = 37 kft, true air speed TAS = 205 m/s, angle of attack AOA = 2.5° and an ice crystal density of 0.918 g/cm^3. The panels are for different particle sizes, indicated in the panels. Ice particles starting at the lowest trajectory position enter the middle inlet tube of the IWC inlet if the particle follows the gas streamline. The simulations are performed by means of CFX 18.2 by ANSYS Inc., for a more detailed description of the methods applied in the simulations see Weigel et al. (2016).

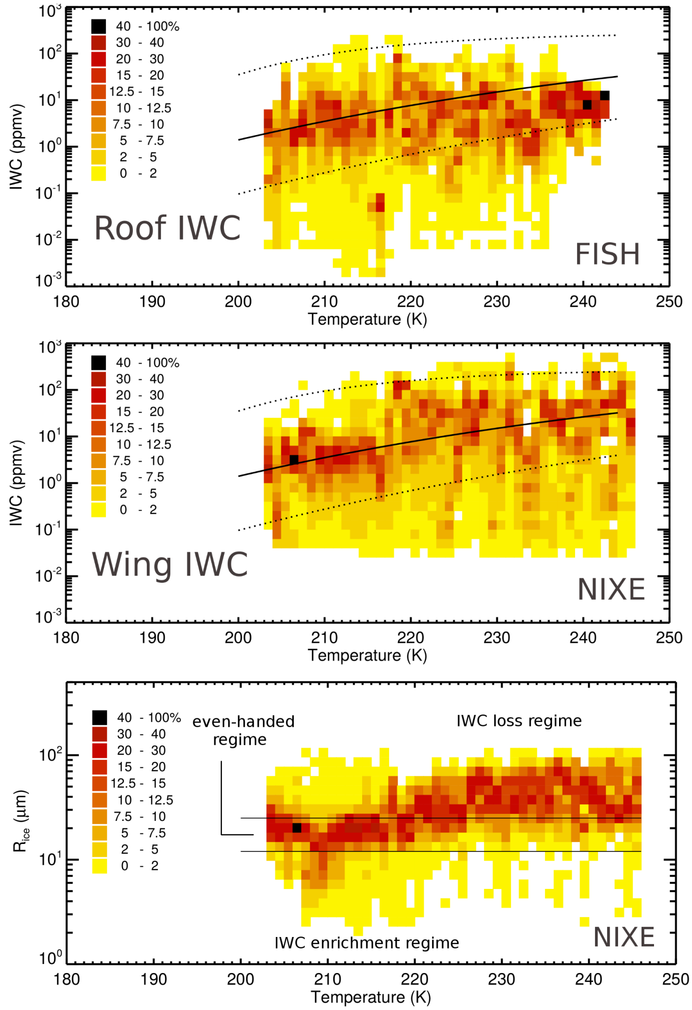

Figure 15. Top and middle panel: IWC and in dependence ~~o~~ of temperature during ML-CIRRUS 2014, from roof-mounted FISH and wing-mounted NIXE (color code: frequencies of occurrence, black solid and dashed lines: median, core min. and max. IWCs after Schiller et al., 2008). Bottom panel: R_{ice} in dependence of temperature during ML-CIRRUS 2014, from wing-mounted NIXE (the black lines denote the size regimes where ice particles are lost, enriched or both, for detail see Section 5.2).